Science of the Total Environment 904 (2023) 166658

Contents lists available at ScienceDirect

Science of the Total Environment

journal homepage: www.elsevier.com/locate/scitotenv

Protecting the invisible: Establishing guideline values for copper toxicity to marine microbiomes

Marie C. Thomas [a,b,c,*], Gretel Waugh [a,b,c], Inka Vanwonterghem [a], Nicole S. Webster [a,b,d], Christian Rinke [a], Rebecca Fisher [e], Heidi M. Luter [b,c], Andrew P. Negri [b,c]

[a] Australian Centre for Ecogenomics, School of Chemistry and Molecular Biosciences, University of Queensland, Brisbane, QLD, 4072, Australia
[b] Australian Institute of Marine Science, Townsville, QLD 4810, Australia
[c] AIMS@JCU, Division of Research and Innovation, James Cook University, Townsville, QLD 4811, Australia
[d] Australian Antarctic Division, Hobart, TAS 7050, Australia
[e] Australian Institute of Marine Science Crawley, Crawley, WA, Australia

HIGHLIGHTS

- Evaluation of changes in marine microbial communities under chronic copper exposure
- Low concentrations of copper affect community composition, richness, and diversity
- Novel metrics for microbiome thresholds were proposed.
- *Microbiome* hazard concentrations for copper < current water quality guidelines
- Methods offer opportunity for inclusion of prokaryotes in water quality guidelines

GRAPHICAL ABSTRACT

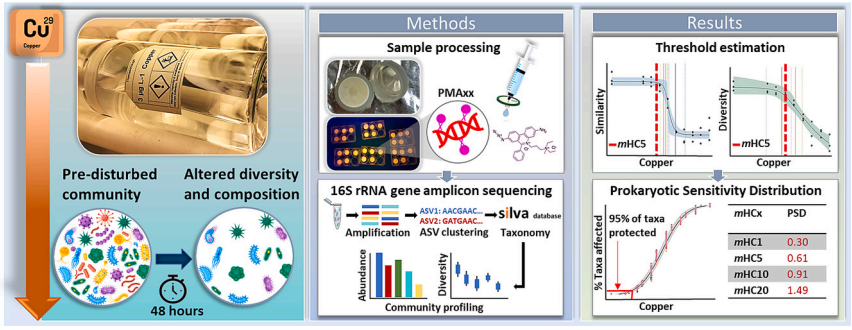

ARTICLE INFO

Editor: Ewa Korzeniewska

Keywords:
Tropical marine microbiome
Copper toxicity
Propidium monoazide
16S
TITAN
Hazard concentration

ABSTRACT

Understanding the rapid responses of marine microbiomes to environmental disturbances is paramount for supporting early assessments of harm to high-value ecosystems, such as coral reefs. Yet, management guidelines aimed at protecting aquatic life from environmental pollution remain exclusively defined for organisms at higher trophic levels. In this study, 16S rRNA gene amplicon sequencing was applied in conjunction with propidium monoazide for cell-viability assessment as a sensitive tool to determine taxon- and community-level changes in a seawater microbial community under copper (Cu) exposure. Bayesian model averaging was used to establish concentration-response relationships to evaluate the effects of copper on microbial composition, diversity, and richness for the purpose of estimating *microbiome* Hazard Concentration (*m*HCx) values. Predicted *m*HC5 values at which a 5 % change in microbial composition, diversity, and richness occurred were 1.05, 0.72, and 0.38 μg Cu L^{-1}, respectively. Threshold indicator taxa analysis was applied across the copper concentrations to identify taxon-specific change points for decreasing taxa. These change points were then used to generate a Prokaryotic Sensitivity Distribution (PSD), from which $mHCx_{dec}$ values were derived for copper, suitable for the protection of 99, 95, 90, and 80 % of the marine microbiome. The $mHC5_{dec}$ guideline value of 0.61 μg Cu L^{-1}, protective of 95

* Corresponding author at: Australian Centre for Ecogenomics, School of Chemistry and Molecular Biosciences, University of Queensland, Brisbane, QLD 4072, Australia.
E-mail address: marie.thomas@uq.net.au (M.C. Thomas).

https://doi.org/10.1016/j.scitotenv.2023.166658
Received 11 July 2023; Received in revised form 24 August 2023; Accepted 26 August 2023
Available online 1 September 2023

% of the marine microbial community, was lower than the equivalent Australian water quality guideline value based on eukaryotic organisms at higher trophic levels. This suggests that marine microbial communities might be more vulnerable, highlighting potential insufficiencies in their protection against copper pollution. The *m*HCx values proposed here provide approaches to quantitatively assess the effects of contaminants on microbial communities towards the inclusion of prokaryotes in future water quality guidelines.

1. Introduction

1.1. Marine microbial communities in environmental risk assessments

Marine microbial communities play pivotal roles in maintaining the functioning, health, and resilience of high-value ecosystems, including coral reefs (Ainsworth et al., 2010; Bourne and Webster, 2013; Maher et al., 2022). However, these communities are highly sensitive to environmental perturbations and disturbance events, such as changes in sea surface temperature and water quality, which can alter the microbial community structure and functionality (Allison and Martiny, 2008; Cavicchioli et al., 2019; Nogales et al., 2011; Vanwonterghem and Webster, 2020). Estimating disturbance-related deviations from the natural community composition could therefore provide an early warning for declining reef health and enable sensitive predictions of environmental stress (Astudillo-García et al., 2019; Glasl et al., 2018; Glasl et al., 2017; McDevitt-Irwin et al., 2017). Free-living microbial communities, in particular, have a high potential for inferring environmental fluctuations compared to host-associated communities due to their high uniformity and environmental sensitivity (Glasl et al., 2019).

Considerable efforts have been made towards unravelling the spatial and temporal dynamics of marine microbial communities. For instance, the Australian Marine Microbial Biodiversity Initiative represents a standardized ocean observatory program that provides a comprehensive amplicon sequencing database for describing microbial community dynamics across Australia's marine ecosystems (Brown et al., 2018). Yet, despite the evidence that microbial communities often possess limited resistance, resilience, and functional redundancy in response to environmental change than previously thought (Allison and Martiny, 2008; Bissett et al., 2013), management guidelines aimed at protecting aquatic organisms from environmental pollution remain primarily defined for organisms at higher trophic levels (e.g., fish, invertebrates, molluscs or algae) (Cavicchioli et al., 2019; Webster et al., 2018). Describing the impacts of environmental stress on microbial communities is generally based on qualitative terms, primarily due to the inability of current ecotoxicology methodologies to establish quantitative stress-response relationships to inform the development of regulatory guidelines (Hazen, 2020; Webster et al., 2018). Establishing a regulatory framework capable of predicting environmentally relevant risk thresholds for marine microbiomes would allow for timely management interventions to mitigate the impact of human activities well before coral reef health deteriorates (Glasl et al., 2018; Webster et al., 2018).

1.2. Water quality guidelines for the protection of aquatic organisms

Water quality guideline values refer to the maximum acceptable concentrations of contaminants in aquatic environments that are protective of aquatic organisms (USEPA, 2019). These guideline values are often derived from toxicity threshold data from diverse species modelled as cumulative Species Sensitivity Distributions (SSD) against the contaminant concentration. This approach enables estimation of the proportion of species in a community that would be affected by different concentrations of contaminants (Posthuma et al., 2019). For example, a concentration hazardous to 5 % of a community is referred to as the HC5 (in Australia and New Zealand, this is equivalent to the Protective Concentration PC95) (ANZG, 2018). Several statistical methods have been applied to predict toxicity thresholds used to derive SSDs; however, the preferred statistical estimates include No Effect Concentrations (NEC) (Fox, 2010) and x% Effect/Lethal Concentrations (EC/LCx; where $x \leq 10$) generated from chronic exposure experiments (Warne et al., 2018). The SSD approach has been applied globally to investigate relationships among sensitivities of temperate and tropical eukaryotic species to contaminants (e.g., metals, pesticides, hydrocarbons) (ANZG, 2018; CCME, 2005; EFSA, 2013; USEPA, 2019) but have not been developed for prokaryotes. Accounting for microbial sensitivities in water quality guidelines requires novel approaches to define toxicity thresholds for the entire community that meet established ecotoxicological criteria and are suitable for application in, or comparison with, an SSD.

1.3. Quantifying microbial responses to environmental stress

Assessing microbial responses to environmental stress at both compositional and functional level has historically been challanged by the need to account for high microbial abundance, diversity, functional complexity, and low cultivability (Allison and Martiny, 2008; Bissett et al., 2013). Ecotoxicology methodologies are generally restricted to testing a limited range of laboratory cultured bacterial strains and quantifying direct inhibitory effects on microbial growth, biomass, or luminescence of a single test species (e.g., Microtox assay) (Shahsavari et al., 2017). However, contaminants may elicit complex direct and indirect responses that differ among taxa in the community, subsequently leading to a decline in species richness, diversity and changes of community structures or network associations. This shift will often have repercussive impacts on the entire community and ecosystem, highlighting the requirement for data representative of the community-level rather than single isolates (Bissett et al., 2013; Zhang, 2019). Community-level impacts of contaminants on eukaryotic communities have been explored using mesocosms and microcosms for decades (Caquet et al., 2000) and with the advances in next-generation sequencing, it is now possible to assess microbial responses across the phylogenetic biodiversity of entire communities within highly controlled experimental microcosm systems (Webster et al., 2018).

These approaches provide the necessary information for (microbial) ecotoxicology to establish concentration-response relationships such that quantitative microbial data can be integrated into standard toxicity testing, regulatory, and management guidelines (Birrer et al., 2017; Webster et al., 2018). For instance, Doolette et al. (2016) applied a combination of quantitative PCR and 16S rRNA gene amplicon sequencing to derive toxicity thresholds for soil microbial communities that respond negatively to silver. These toxicity values were combined in an SSD to derive HCx values for silver to the microbial soil community. Such approaches present a tremendous opportunity to enhance our quantitative understanding of stress-induced alterations in microbial communities that play crucial roles in driving global biogeochemical cycles and maintaining ecosystem health.

The objective of this study was to apply established principles of ecotoxicology to 16S rRNA gene amplicon sequence data to identify thresholds for taxon- and community-level changes in a seawater microbial community exposed to copper (Cu). In the context of preforming ecotoxicology testing, the distinction of intact cells from membrane compromised cells is essential as concentration-response modelling should only include viable community members. For this purpose, samples were treated with propidium monoazide (PMA) – a selective dye that penetrates membrane compromised cells allowing covalent cross-linkage to DNA upon light exposure. The covalent binding of the

dye to the DNA results in a strong inhibition of PCR amplification (Nocker et al., 2007).

Copper was selected as a reference toxicant as its most bioavailable form (dissolved Cu^{2+}) is widely reported to be one of the most toxic metals to aquatic organisms (Solomon, 2008). Usually present in the marine environment at <1 μg Cu L^{-1} (Apte et al., 2017), elevated copper concentrations are directly related to urban and industrial activities, mine tailings, and the use of antifouling paints on ship hulls (Haynes and Johnson, 2000; Thomas and Brooks, 2010; Warne and Reichelt-Brushett, 2023). Although its application is increasingly regulated (Warne and Reichelt-Brushett, 2023), copper remains among the most frequently detected metals in tropical marine environments, including nearshore surface waters of the Great Barrier Reef at concentrations up to 3.9 μg Cu L^{-1} (Kroon et al., 2015).

Our first approach applied Bayesian model averaging to establish concentration-response relationships and estimate toxicity thresholds as measures of effect on microbial composition, richness, and diversity. Our second approach involved the development of an SSD-like *Prokaryotic Sensitivity Distribution* (PSD) from change points identified using Threshold Indicator Taxa ANalysis (TITAN). This allowed the derivation of *microbiome* Hazard Concentration (*m*HCx) values below which 99, 95, 90, 80, and 50 % of marine microbial taxonomic groups may be protected from copper pollution. The *m*HCx values can be assessed against HCx values generated from traditional SSDs, allowing comparisons in community sensitivity between prokaryotic and eukaryotic communities. Proposed metrics that describe thresholds for change in communities of mixed microorganisms in response to contaminants are summarized in Table 1.

2. Methods

2.1. Preparation of copper stock solutions

All experimental plastic containers were subjected to acid-washing using 10 % (*v*/v) hydrochloric acid and subsequently rinsed several times with demineralised water, and then with ultra-pure water (18.2 MΩ·cm, Milli-Q IQ 7000, Merck). Copper parent stocks of 1 and 100 mg Cu L^{-1} were prepared in Milli-Q water from copper (II) chloride (anhydrous $CuCl_2$, CAS 7447-39-4, HPLC ≥97 %, Honeywell Riedel-de-Haën, Germany) in 1 L clear polyethylene terephthalate jars (Synergy Packaging, Australia). The working stocks that were used for copper dosing in the 48-h experiment were dilutions of the parent stocks in Milli-Q water. The range of copper concentrations (nominal concentrations: 0, 0.1, 0.3, 1, 3, 10, 30, 100, 300, 1000 μg L^{-1}) selected for experiments were based upon available data for copper toxicity to marine species from the US Environmental Protection Agency ECOTOX database (USEPA, 2019). The higher copper treatments were chosen to capture the full concentration-response relationship. Total and dissolved copper was measured across the treatments as described in the Supplementary Information.

2.2. Seawater collection

Inshore seawater was collected during high tide from a jetty (19°16′38.4"S, 147°03′32.1"E) located at the Australian Institute of Marine Science, Townsville QLD in December 2020. Seawater was collected with a submersible pump (750 GHP, Rule-Mate, Xylem Inc., USA) at 1 m depth and subsequently pre-filtered with 25 and 5 μm polyester filter bags (Waterco, Australia). All samples were immediately stored in the dark at 26°C, consistent with the sea surface temperature at the time of collection, until further processing.

2.3. Experimental set-up for copper exposure

Three replicate 1 L polyethylene terephthalate jars were filled with 946 mL of 5 μm filtered seawater across each of the 10 copper treatment concentrations ($n = 30$). Immediately prior to copper addition (referred to as timepoint 0 h thereafter), 50 mL subsamples were taken in duplicate from each replicate treatment jar using sterile 50 mL TERUMO syringes (see below for filtration details). Replicate jars were then spiked with a range of copper concentrations (by adding 4 mL aliquots from each working stock to individual jars) and firmly sealed leaving a 10 % headspace to allow for oxygen exchange. Jars were randomly placed horizontally on rollers at 40 rpm for aeration movement during the exposure period and incubated at 27.3 ± 0.7°C (mean ± SD) under a 12:12 h light:dark cycle at 160–180 μmol photons m^{-2} s^{-1} (Osram Lumilux Cool White 36 W) until sampling at later timepoints. An additional set of 10 jars (water quality jars) containing identical volumes of filtered seawater and copper concentrations as explained above, were incubated in the same manner to allow for water quality measurements and collection of chemical samples without potential contamination.

Table 1
Summary of threshold definitions for the effect of copper on the marine microbiome. *Microbiome* Hazard Concentrations (*m*HCx) represent x% change for each metric in comparison to the control community (0.18 μg Cu L^{-1}). The microbiome community thresholds are referred to as Hazard Concentrations rather than Effect Concentrations (ECx) which are routinely applied to single species. *m*HCx values represent thresholds for change in the community which can be influenced by interspecific interactions among taxa, in contrast to HCx values derived from Species Sensitivity Distributions (SSDs) of (mostly) eukaryotic species tested independently. Threshold Indicator Taxa ANalysis (TITAN) community change points are also included for comparison.

Threshold	Data *Method*	Definition
$\boldsymbol{m}$**HCx$_{sim}$**	Bray-Curtis similarity *Concentration-response model:* ***C-R$_{sim}$***	Concentration at which the community composition differs from that of the control community by x%.
$\boldsymbol{m}$**HCx$_{div}$**	Shannon diversity *Concentration-response model:* ***C-R$_{div}$***	Concentration at which the community diversity differs from that of the control community by x%.
$\boldsymbol{m}$**HCx$_{rich}$**	Observed richness *Concentration-response model:* ***C-R$_{rich}$***	Concentration at which the community richness differs from that of the control community by x%.
$\boldsymbol{m}$**HCx$_{dec}$**	zenv.cps of decreaser ASVs *Cumulative Prokaryotic Sensitivity Distribution:* ***PSD$_{dec}$***	Concentration at which x% of decreaser ASVs reduce in relative abundance and/or frequency based on a cumulative distribution of TITAN change points (zenv.cps). Indicator ASVs selected on purity and reliability criteria (pur.cut/rel.cut ≥0.95).
$\boldsymbol{m}$**HCx$_{all}$**	zenv.cps of all ASVs *Cumulative Prokaryotic Sensitivity Distribution:* ***PSD$_{all}$***	Concentration at which x% of all ASVs change in relative abundance and/or frequency based on TITAN change points (zenv.cps). No purity and reliability criteria applied.
zenv.cps	Relative abundance of ASVs *Indicator species scores across binary sample partitions and bootstrapping:* ***TITAN***	TITAN change points (zenv.cps): concentration at which the greatest change in relative abundance and/or frequency occurs based on normalised indicator values (z-scores).
fsum(z)- **fsum(z)+**	Relative abundance of ASVs *Indicator species scores across binary sample partitions and bootstrapping:* ***TITAN***	Filtered community change points (fsumz.*cp*) of indicator ASVs: concentration at which the largest synchronous (greatest cumulative IndVal z score) decline (fsum(z)-) or increase (fsum(z)+) of indicator ASVs occurs. Indicator ASVs selected based on purity and reliability criteria (pur.cut/rel.cut ≥0.95).

2.4. Seawater filtration and PMA treatment

Subsamples (50 mL) were taken in duplicate ($n = 60$) at relevant timepoints (0-, 2-, 7-, 24-, and 48-h) from each treatment jar using sterile 50 mL syringes and connected to sterile 25 mm polypropylene Swinnex filter holders (Millipore, Australia). Seawater samples were filtered onto 25 mm 0.22 μm hydrophilic polyvinylidene fluoride (PVDF) membranes by hand. To limit DNA extraction and PCR amplification to the relevant fraction of the viable community, samples were divided into two sets so that one set could be treated with propidium monoazide (PMA; $n = 30$) to bind extracellular DNA (Nocker et al., 2007), while the other set remained untreated (n = 30). PMA-untreated samples were directly placed into 1.5 mL cryotubes, snap frozen and stored at −80°C. PMA-treated samples were transferred to 6-well plates (Nalge Nunc Int., Denmark) containing 1 mL sterile NaCl solution (0.2 μm filtered). One mL aliquots of PMA stock (PMAxx Dye, 20 mM in H_2O, Biotium, USA) were added to individual wells to final concentrations of 15 μM, conservatively selected to avoid potential PMA-induced cell cytotoxicity at higher PMA concentrations (Banihashemi et al., 2012; Salam et al., 2014; Taylor et al., 2014). Well-plates were incubated in the dark for 10 min before being subsequently light exposed for 10 min using a 464 nm light LED Transilluminator (Clare Chemical, USA) to achieve photo-induced PMA cross-linking to extracellular DNA (Nocker et al., 2006; Nocker et al., 2007). Gentle swirling of the plates was performed periodically to ensure homogeneous light exposure. Membrane filters were then removed from the well plates and transferred to 1.5 mL cryotubes using sterile tweezers. Samples were snap frozen in liquid nitrogen and stored at −80°C. Water quality analysis including pH, salinity, dissolved oxygen, as well as samples for dissolved and total copper and nutrient (dissolved organic/inorganic carbon and nitrogen; < 0.45 μm filtered) analysis were taken for each treatment as described in the Supporting Information.

2.5. DNA extraction and 16S rRNA gene amplicon sequencing

DNA was extracted from filter membranes using a phenol-chloroform extraction method adapted from He (2011). Extracted DNA was resuspended in 30 μL UV-treated Milli-Q water and placed at 4°C overnight. After DNA quantification by NanoDrop 2000 spectrophotometer (Thermo Fisher Scientific, Australia) and Qubit fluorometer (Thermo Fisher Scientific, Australia), DNA samples were stored at −20°C until being sent for library preparation and sequencing to the Australian Centre for Ecogenomics in Brisbane, Queensland. The V1-V3 hypervariable regions of the 16S rRNA gene was amplified using the primer pair 27F (5′-AGAGTTTGATCMTGGCTCAG-3′) (Lane, 1991) and 519R (5′-GWATTACCGCGGCKGCTG-3′) (Turner et al., 1999). Libraries were generated with the 16S Metagenomic Sequencing Library Preparation Protocol (15044223 B) and sequenced on the Illumina MiSeq using 2 × 300 bp paired-end chemistry.

2.6. Sequence processing

Demultiplexed raw sequence data was processed using the QIIME 2 pipeline v2020.8 (Bolyen et al., 2019) using forward reads only due to poor sequence overlap between forward and reverse reads after truncation using a quality score of 30. Amplicon primers were removed with the plugin cutadapt (Martin, 2011). The plugin DADA2 (Callahan et al., 2016) was applied to denoise single-end sequences (truncation of poor-quality bases, dereplication and chimera filtering). Sequences were clustered into features based at 100 % sequence similarity, subsequently referred to as amplicon sequence variants (ASVs). A naïve-Bayes taxonomy classifier was trained against the SILVA v132 99 % OTUs references from the 27F/519R region (Quast et al., 2012) with the feature-classifier plugin (Bokulich et al., 2018). The trained classifier was applied to the representative sequences to assign taxonomy using the classify-sklearn command (Pedregosa et al., 2011) in the feature-classifier plugin. A total of 12,630,500 Illumina sequence reads were recovered across the 300 seawater samples following quality filtering. Unassigned reads, mitochondrial, chloroplast, and eukaryote sequence reads were removed. The remaining 11,869,096 reads (Min: 755, Max: 120,729 read depth) included 22,970 ASVs assigned to 119 prokaryotic classes within 48 phyla. Samples were rarefied to 9500 random reads based on rarefaction curves (Supplementary Fig. S1) indicating that diversity was fully captured in most communities. This resulted in the exclusion of three samples (T7_0_μgL_R3_PMAtreated, T48_23.87_μgL_R1_PMAuntreated, T48_79.57_μgL_R1_PMAuntreated) that did not meet the minimum required number of reads. Demultiplexed sequences and metadata are accessible in the NCBI Sequence Read Archives under BioProject number PRJNA983933.

2.7. Threshold derivations

2.7.1. Microbial diversity and community composition analyses

Statistical analyses were performed using the R Statistical Software environment v4.2.1 (R Core Development Team, 2023). Alpha diversity estimators, as measured by the richness, evenness and Shannon diversity index, were calculated (after rarefaction) using the *phyloseq* R package v1.40.0 (McMurdie and Holmes, 2013). Effects of copper, timepoints, PMA treatment, as well their interactions were tested using a Generalized Linear Mixed Model (GLMM) which was fitted with the Shannon diversity index (normalized by the natural logarithm of the maximum richness index) as the response variable using a beta distribution and logit link function. The main fixed factors were PMA, timepoint, and copper while using sample jars as a random factor. Modelling was done with the *glmmTMB* R package v1.1.5 (Brooks et al., 2017). Distribution of simulated residuals was assessed with the *DHARMa* R package v0.4.6 (Hartig, 2022). The *MuMIn* R package v1.47.1 (Barton and Barton, 2015) was used to identify the best candidate model(s) built with all possible combinations of explanatory variables. Model(s) were selected based on Akaike Weights and Akaike Information Criterion (AIC). Planned contrast matrices were generated with the *emmeans* R package v 1.8.4–1 (Lenth et al., 2023) to test for the effects of copper on microbial diversity at different timepoints and for both PMA-treated and PMA-untreated communities. Results from the pairwise contrasts were reported with t-ratios and *p*-values (adjusted using a "mvt" correction for multiple comparisons).

Beta diversity analysis was performed using Bray-Curtis dissimilarity matrices based on Hellinger transformed abundance data. Principal coordinate analysis limited to the first two dimensions was employed to visualize the microbial community composition using the *phyloseq* R package. Permutational Multivariate Analysis of Variance (PERMANOVA), pair-wise comparison, as well as Multivariate Homogeneity of Group Dispersion (PERMDISP2) was calculated in PRIMER v7.0.21 (Clarke and Gorley, 2015) to test for differences in community structure between copper concentrations, timepoints and PMA treatments. All visualization plots were generated using the *phyloseq* R packages in conjunction with the *ggplot2* R package v 3.4.0 (Wickham, 2016).

2.7.2. Fitting concentration-response curves

Microbiome Hazard Concentrations (*m*HCx) values were estimated from concentration-response curves generated in the *bayesnec* R package v2.1.0.2 (Fisher et al., 2023) using the decreasing Bray-Curtis similarity, richness, and Shannon diversity indices as beta-, poisson-, and gamma-distributed response variables, respectively, against the logarithmic copper concentrations. The package uses Hamiltonian Monte Carlo chains and supports multi-model fitting with Bayesian model averaging which is achieved through a weighted sample of each fitted models' posterior predictions (Vehtari et al., 2017). The control community was thereby defined as samples at concentration of 0.18 μg Cu L^{-1}, so that the similarity, richness, or diversity values at 0.18 μg Cu L^{-1} are an estimation of the variability between replicated control samples. We assumed that the Bray-Curtis similarity, richness, and diversity indices

could theoretically reach a minimum value close to zero (Arbel et al., 2015) and therefore an absolute x% decline was bounded between the upper asymptote (control treatment) and zero. The modelled response of Bray-Curtis similarity, richness, and diversity indices were restricted to the initial decline at ecologically realistic concentrations. Chain mixing was evaluated visually for convergence. Posterior estimates were calculated using weighted model averaged estimates obtained from all successfully fitted models (model fit statistics and weights for each response variable can be found in the Supplementary Table S1). Model weights were estimated using the pseudobma method with Bayesian bootstrap (Vehtari et al., 2017) via the *loo* R package v2.6.0 (Vehtari et al., 2023).

2.7.3. Threshold Indicator Taxa ANalysis: TITAN

Threshold Indicator Taxa ANalysis (TITAN) can be employed to identify changes in taxa distributions across an environmental gradient and assesses synchrony among taxa change points as evidence for community thresholds (Baker and King, 2010). TITAN applies indicator species scores to identify taxa change points at concentrations where the greatest change in abundance or frequency occurs (using optimal observation partitioning) based on normalised indicator values (z-scores) (Baker and King, 2010). TITAN was performed on relative abundance data, with minSlt = 5; 1000 permutations, 1000 bootstraps, and pur.cut/rel.cut = 0.95 using the *TITAN2* R package v2.4.1 (Baker et al., 2022). Only ASVs present in at least three samples were included in the analysis ($n = 697$ ASVs) to satisfy data requirements for *TITAN2*. TITAN then performed bootstrapping and indicator species analysis to detect community-level change points, as well as ASV-specific change points in response to increasing copper concentrations. Bootstrapping analysis was used to identify only ASVs with consistently strong increasing or decreasing response in ≥95 % (reliability and purity cut off value) of bootstrapped replicates. ASVs that decreased or increased in relative abundance and/or frequency were subsequently defined as "decreasers" and "increasers", respectively. A Sankey diagram was generated with the *networkD3* R package v0.4 (Allaire et al., 2017) to depict taxonomic affiliation and the number of reliable and pure indicators (e.g., purity and reliability scores ≥0.95 of the bootstrap replicates achieving $p \leq .05$). Scatterplots with smoothed line using the Generalized Additive Model (GAM) method were generated with *ggplot2* to visualize changes in the relative abundance (%) of indicator ASVs to increasing copper concentrations.

2.7.4. Prokaryotic Sensitivity Distribution

The *ssdtools* R package v1.0.2 (Thorley and Schwarz, 2018) was used to generate a cumulative *Prokaryotic Sensitivity Distribution* (PSD) based on TITAN-derived change points of all ASVs (no purity and reliability criteria applied) or ASVs identified by TITAN as decreasers (ASVs with pur.cut/rel.cut ≥0.95). *m*HCx values were derived from the PSD representing the concentrations of copper at which x% of ASVs were affected. The *ssdtools* package employs Maximum Likelihood to fit multiple distribution averages and provides model averaged *m*HCx values based on AICc model weights. Confidence intervals on *m*HCx and proportions were estimated by parametric bootstrapping. Distributions selected to use in the candidate model set included the gamma, log-normal, log-logistic, log-Gumbel, Weibull, and log-normal/log-normal distributions.

3. Results

3.1. Experimental conditions

Measured dissolved copper concentrations (< 0.45 μm-filtered, time averaged between 0-h and 48-h) were used in concentration-response modelling. Concentrations below the limit of reporting (< 0.7 μg L^{-1}) were derived via regression analysis ($R^2 = 0.9996$) between the nominal and measured values up to 30 μg L^{-1} (to maximise linearity across the lower, most relevant concentration range) (Supplementary Fig. S2 and Table S2).

The water quality parameters monitored in the seawater of the water quality jars remained within acceptable ranges throughout the experimental exposure period. The variations in dissolved oxygen (DO), pH, and salinity were <5 % (mean ± SD: DO 7.9 ± 0.2 mg L^{-1} (99.4 ± 0.6 %), pH 8.5 ± 0.1, salinity 36.3 ± 0.1 PSU) (Supplementary Table S3). The concentrations of dissolved organic carbon (DOC) and total nitrogen (TN) in the filtered seawater (< 0.45 μm-filtered) at the start of the experiment (0-h) were (mean ± SD) 2.5 ± 0.17 μg L^{-1} and 0.14 ± 0.01 μg L^{-1}, respectively. After 48-h, the concentrations of DOC and TN were 4.4 (3.0– 7.3) ± 1.5 μg L^{-1} and 0.10 (0.09– 0.15) ± 0.02 μg L^{-1}, respectively. Detailed measurements of dissolved inorganic nutrients (NH_4, PO_4, $NO_3 + NO_2$, SI), TN, and DOC can be found in the Supporting Information (Supplementary Table S4).

3.2. Response of the seawater microbiome to copper

The effects of copper on the seawater microbiome were first assessed across sampling timepoints (0-, 2-, 7-, 24-, 48-h) and between PMA-treated and PMA-untreated communities by comparing changes in the average relative abundance, alpha and beta diversity (Fig. 1). Community profiles of the initial control microbiome at 0-h (0.18 μg Cu L^{-1}) showed uniform community assembly patterns between the PMA-treated and PMA-untreated communities (Fig. 1A); however, PMA treatment resulted on average in 42.6 % lower DNA yields (mean ± SD: 2.79 ± 0.71 ng μL^{-1}, $n = 30$) compared to DNA yields of PMA-untreated samples (mean ± SD: 4.86 ± 1.50 ng μL^{-1}, n = 30), suggesting signals from relic DNA were reduced in PMA-treated communities without compromising the viable cell proportion. Overall, taxa of the classes Alphaproteobacteria and Gammaproteobacteria (phylum Proteobacteria), Bacteroidia (phylum Bacteroidetes), and Oxyphotobacteria (phylum Cyanobacteria) were most dominant and accounted for 73–90 % of the control microbiome across all timepoints (Fig. 1A). Classes with low average relative abundance (< 5 %) included Planctomycetacia and OM190 (phylum Planctomycetes), Verrucomicrobiae (phylum Verrucomicrobia), Deltaproteobacteria (phylum Proteobacteria), and Acidimicrobiia (phylum Actinobacteria) (Fig. 1A). In the copper exposed communities, an effect of copper on the community structure of PMA-treated communities could already be observed 2-h after exposure (Fig. 1A). For example, the average relative abundances of Bacteroidia and Gammaproteobacteria mostly increased, while the proportion of Alphaproteobacteria and Oxyphotobacteria decreased compared to the control microbiome (Fig. 1A). In contrast, there was little change with increasing copper concentrations in the average relative abundance of taxa in the PMA-untreated communities until 24-h (Fig. 1A). In part, this might be explained by the presence of membrane-compromised cells that were retained in the PMA-untreated samples and amplified during PCR prior to sequencing. However, marked changes in average relative abundances of Bacteroidia and Gammaproteobacteria in both PMA-treated and PMA-untreated communities were observed at 48-h. These taxa increased by up to 50 % and 44 %, respectively, relative to the control microbiome at mid-range copper concentrations, but decreased by as much as 44 % and 26 %, respectively, at higher concentrations (Fig. 1A). Conversely, Alphaproteobacteria showed a decline in their average relative abundance at lower and mid-range concentrations (up to 83 % relative to the control microbiome), and then increased by as much as 18 % at a concentration of 788 μg Cu L^{-1} (Fig. 1A).

Diversity metrics were then used to explore the effects of increasing copper concentrations on microbial diversity (Fig. 1B). The Shannon diversity index remained consistent in the control microbiome across timepoints and there was little variation for both PMA-treated (mean ± SD: 4.92 ± 0.13, $n = 14$) and PMA-untreated (mean ± SD: 4.71 ± 0.10, $n = 15$) communities (Fig. 1B). However, alpha diversity varied greatly between the control and copper exposed microbiomes ($\chi^2(9) = 196.13$, $p < .001$, Supplementary Table S5), with PMA-treated communities indicating a significantly higher microbial diversity than the PMA-

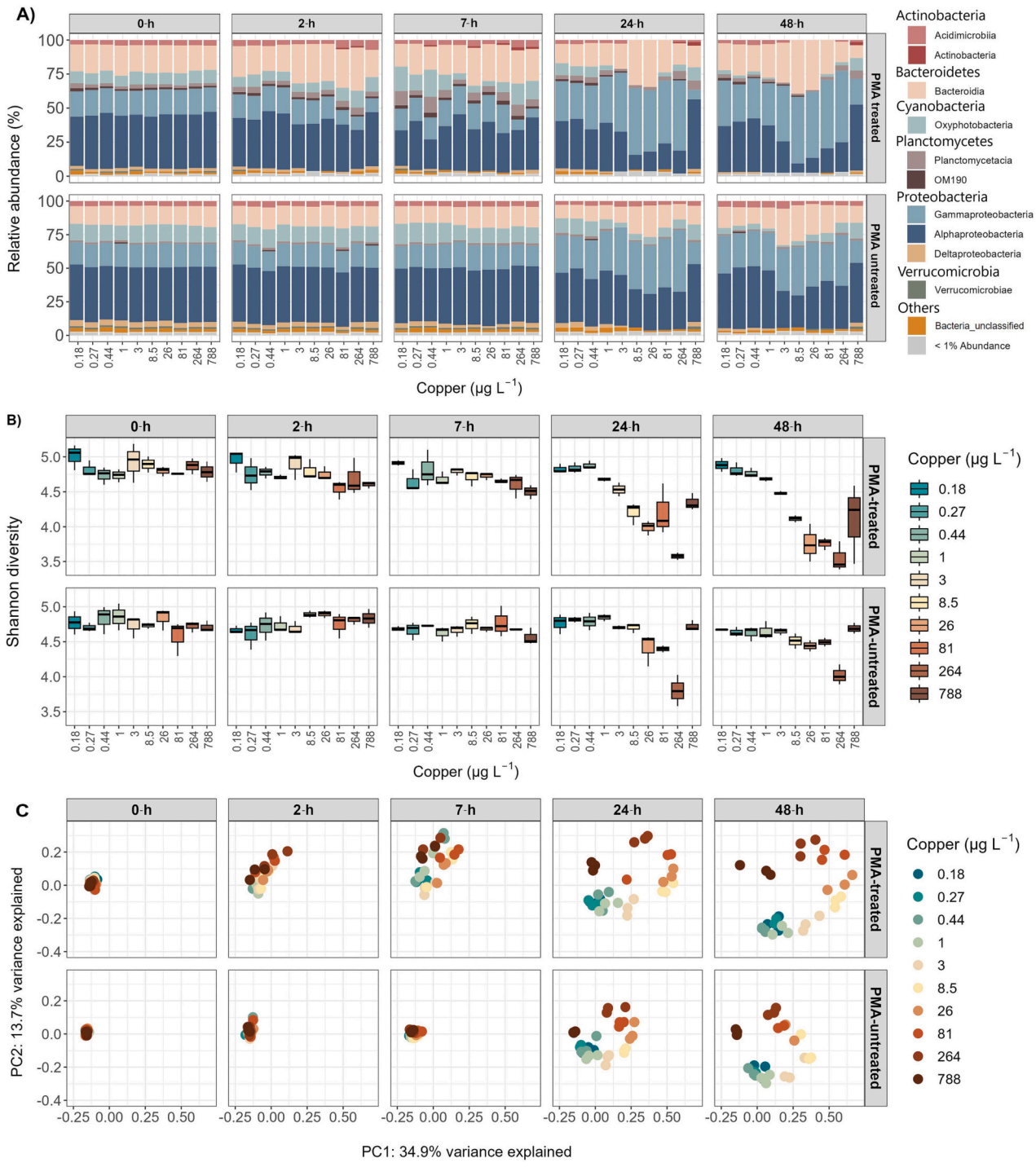

Fig. 1. Seawater microbiome responses following exposure to ten copper concentrations (n = 3 replicates) over five timepoints up to 48-h. Note that samples collected at timepoint 0-h were obtained prior to the addition of copper. A) Average relative abundance of the microbial community at class level (grouped by phyla). B) Boxplot of Shannon diversity index (n = 3 replicates). The whiskers symbolize the 10th and 90th percentiles, the box denotes the 25th and 75th percentiles, and the horizontal line indicates the median. C) Principal coordinate analysis based on Bray-Curtis dissimilarities at amplicon sequence variant level (n = 3 replicates). In the top series of each panel, samples were treated with propidium monoazide (PMA) post sampling, while samples of the lower series remained untreated.

untreated communities ($\chi^2(1) = 14.51$, $p < .001$, Supplementary Table S5). For example, in the PMA-treated communities, copper significantly affected alpha diversity already at 2-h exposure (t-ratio (230) = 4.01, $p < .001$, Supplementary Table S6), while diversity of the PMA-untreated communities was largely unaffected until 24-h (t-ratio (230) = 4.70, $p < .001$, Supplementary Table S6). The greatest decline (26 % relative to control) in alpha diversity was observed at 48-h which was greater for the PMA-treated communities and post hoc pairwise contrasts identified that communities exposed to concentrations of ≥3 µg Cu L^{-1} had a significantly lower diversity compared to the control microbiome (t-ratio(230) = 3.47, $p = .022$, Supplementary Table S7). Similarly, for PMA-untreated communities, concentrations of ≥26 µg Cu L^{-1} had a significantly lower diversity compared to the control microbiome (t-ratio(230) = 5.55, $p < .001$, Supplementary Table S7). Notably, there were apparent increases in diversity at the highest concentration of 788 µg Cu L^{-1} for both communities (potentially explained

by an increase in dissolved organic carbon; Supplementary Table S4 & Fig. 1B).

The variability in microbial community profiles was further summarized at the ASV-level by investigating the effects of copper on compositional dissimilarities (Bray-Curtis dissimilarity) (Fig. 1C). When analysing the control microbiomes of both PMA-treated and PMA-untreated samples at different timepoints, principal coordinate analysis (PCoA) displayed clear clusteringof both communities, and no significant compositional dissimilarities were detected between communities within each timepoint (PERMANOVA, PMA:timepoint $p >$ .05, Supplementary Fig. S3). However, with increasing exposure duration PCoA revealed a progressive separation of communities, with copper exposure accounting for most of the observed dissimilarities, explaining 48.6 % of the variation in the first two principal coordinates (PCs) (Fig. 1C). Both PMA-treated and untreated communities experienced significant changes in response to copper exposure over 48-h relative to the control microbiome (PERMANOVA; Supplementary Table S8: treatment*timepoint*PMA). In particular, significant shifts in the composition of PMA-treated communities occurred at 7-h copper exposure and all subsequent time points (Supplementary Table S9), whereas no significant composition changes were observed in the PMA-untreated communities until 24-h (Supplementary Table S9). Like the relative abundance profiles and alpha diversity, the strongest community shift occurred at 48-h, which was more evident for the PMA-treated communities and pairwise comparisons revealed that communities exposed to ≥3 μg Cu L^{-1} had significantly different community compositions than the control microbiome (Supplementary Table S10).

3.3. Concentration-response relationships for microbial community similarity, richness, and diversity

In order to derive chronic copper toxicity thresholds for seawater microbiomes, concentration-response relationships were established based on Bray-Curtis similarity (as a metric of community composition change), observed ASV richness and Shannon diversity data (Supplementary Tables S11 & 12). According to the Australian Water Quality Guideline Values, an exposure duration of >24 h is considered chronic for microorganisms (Warne et al., 2018). Therefore, x% changes were only assessed for communities exposed to copper for 48-h and treated with PMA to only include the response of "viable" community members.

Consistent with the analysis that included all timepoints and communities (PMA-treated and PMA-untreated) (Fig. 1), unconstrained ordination (PCoA based on Bray-Curtis dissimilarities) supported a distinct grouping of the PMA-treated communities according to copper concentrations. The first two PCs explained 65.7 % of variation, and clustering patterns showed significant dissimilarities (PERMANOVA, $F(9, 20) = 4.34$, $p < .001$, permutations = 9999) between copper exposures (Fig. 2A), but there was no significant difference in multivariate dispersion among replicates from the same copper concentrations (PERMDISP2, $F(9,20) = 2.00$, $p = .09$, permutations = 9999).

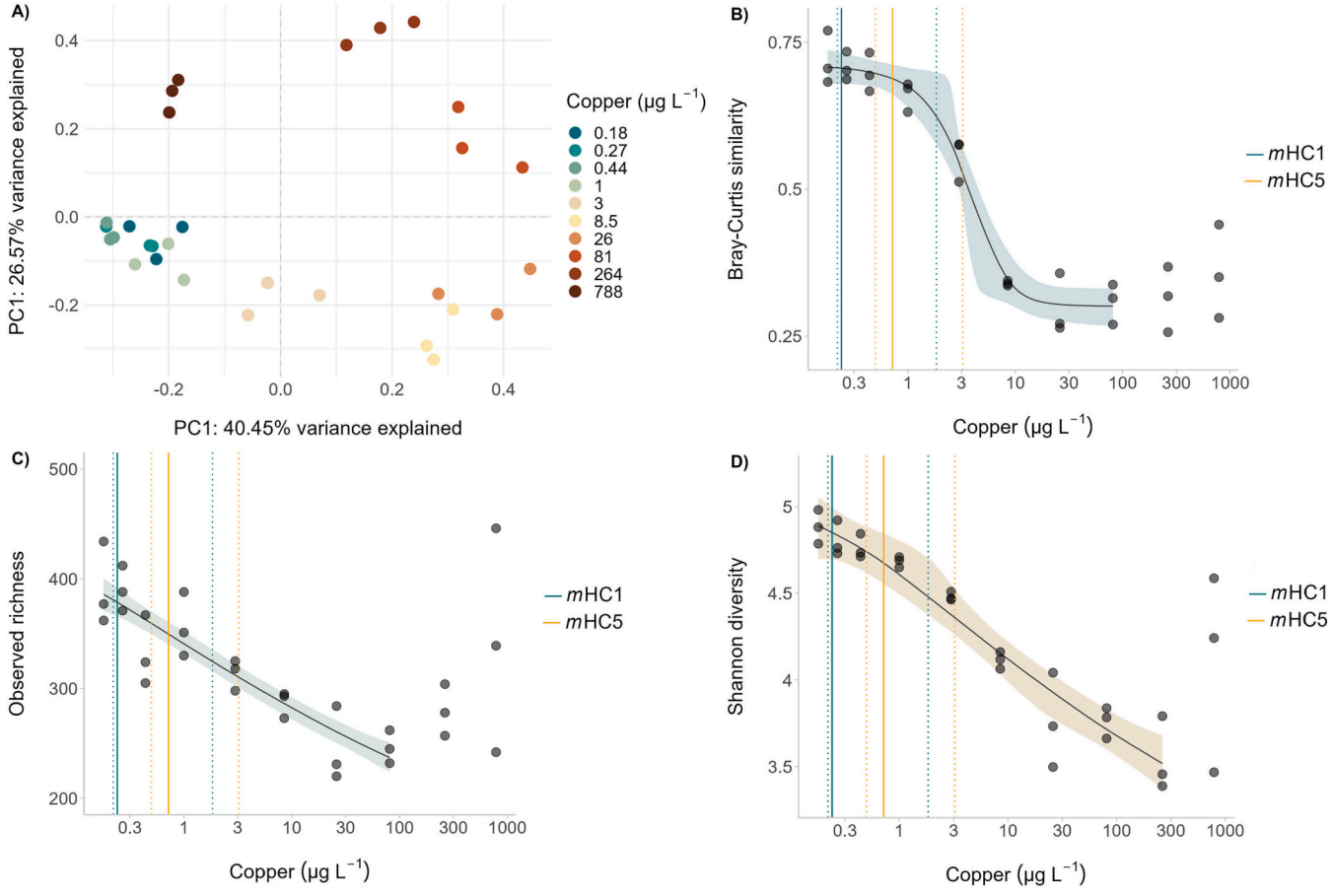

Fig. 2. Derivation of *microbiome* Hazard Concentrations (*m*HCx). A) Principal coordinate analysis based on Bray-Curtis dissimilarities at amplicon sequence variant (ASV) level for seawater microbiomes exposed to 10 copper concentrations at 48-h and treated with propidium monoazide (PMA) post sampling. (B—D) Modelled responses for community similarity, richness and diversity of seawater microbiomes exposed to 10 copper concentrations at 48-h and PMA treatment post sampling: Modelled concentration-response curve based on B) Bray-Curtis similarity, C) observed ASV richness and D) Shannon diversity. The *m*HCx represent x% change for each metric in comparison to the control community (0.18 μg Cu L^{-1}). The dark cyan line represents a 1 % change relative to control, while the orange line equals a 5 % change. Dotted lines show 95 % confidence intervals (CI). Individual fitted responses were restricted to concentrations at which a strict decline was observed. Shading represents 95 % model CI (n = 3 replicates). Note differences in y-axis scaling for individual figures.

Changes in community similarities due to increasing copper concentrations followed an initial sigmoidal decline, allowing estimates of thresholds at which x% change in community similarities occurred (Fig. 2B & Table 2). There was a substantial change in the community structure across concentration ranges of 1 to ~30 μg Cu L^{-1}, after which the community similarity became more stable across the remainder of the concentration series (indicating a potential asymptote). While we cannot predict the response beyond the highest exposure concentration, the similarity can theoretically reach zero as concentrations increase further. The models were therefore restricted to concentrations at which a strict decline relative to the control could be observed, estimating mHC1$_{sim}$ and mHC5$_{sim}$ values of 0.44 and 1.05 μg Cu L^{-1}, respectively (Table 2). ASV richness and Shannon diversity followed similar declines with increasing copper concentrations, again showing evidence of lower plateaus or increases at very high concentrations (Fig. 2C&D). The mHC5$_{rich}$ and mHC5$_{div}$ were 0.38 and 0.72 μg Cu L^{-1}, respectively (Table 2).

3.4. Identification of microbial indicator taxa using TITAN

Threshold Indicator Taxa ANalysis (TITAN) identified change points corresponding to copper concentrations at which the greatest increase or decrease in the relative abundance/and or frequency occurred for each ASV (subsequently referred to as increasers or decreasers, respectively) in the PMA-treated community after 48-h exposure. The indicator ASVs that met the criteria for purity and reliability (≥ 0.95, $p < .01$) are plotted in Fig. 3, along with their taxon-level change points (values of copper resulting in the largest indicator z value) that are visualized as a probability density function of the bootstrapped replicates (nBoot = 1000). A total of 197 decreaser (28 %) and 63 increaser (9 %) ASVs were detected as significant indicators for copper (Fig. 3, Supplementary Table S4). These indicator ASVs accounted for 37 % of the prefiltered community (= 697 ASVs; prefiltered community representing ASVs that were present in at least three samples). The filtered sum of change points fsum(z)- was 5.75 μg Cu L^{-1}, representing the copper concentration at which the greatest synchronous decline in the relative abundances and/or frequencies of ASVs in the indicator seawater microbiome occurred (Fig. 3, Supplementary Table S13). Conversely, the greatest synchronous increase (fsum(z)+) was observed at a concentration of 17.3 μg Cu L^{-1} (Fig. 3, Supplementary Table S13).

3.5. Comparison of relative taxon-specific changes

Taxonomic analysis of the indicator ASVs identified by TITAN was used to illustrate the distribution of decreaser and increaser ASVs among the various taxonomic levels (Fig. 4A). Out of 22 total classes, decreaser ASVs were found in 13 classes, whereas increaser ASVs were observed in only 8 classes (Fig. 4A). These taxa demonstrated clear concentration-dependent trends, with decreaser ASVs showing declines and increaser ASVs displaying increases in the relative abundance with increasing copper concentrations (Fig. 4B).

The classes Alphaproteobacteria, Gammaproteobacteria (phylum Proteobacteria) and Bacteroidia (phylum Bacteroidetes) were largely represented by taxa identified as both decreasers and increasers (Fig. 4A). However, taxa from the classes Deltaproteobacteria (phylum Proteobacteria), OM190 (phylum Planctomycetes), and Acidimicrobiia (phylum Actinobacteria) consisted exclusively of decreasers, while the class Mollicutes (phylum Tenericutes) exclusively included increasers (Fig. 4A). Within Alphaproteobacteria and Gammaproteobacteria, several orders demonstrated a high prevalence of consistently identified decreasers. These orders included SAR11 clade, Parvibaculales, Oceanospirillales, Cellvibrionales, SAR89 clade, and OM182 clade (Fig. 4A). Conversely, the orders Rhodobacterales and Alteromonadales contained both indicators but with a higher proportion of decreasers (Fig. 4A). Among the Bacteroidia, taxa from the orders Chitinophagales and Cytophagales only compromised decreasers, whereas Flavobacteriales included both indicators (Fig. 4A). Taxa affiliated with orders Synechococcales and Acholeplasmatales were the only orders primarily consisting of increasers (Fig. 4A). Non-indicator ASVs were distributed across most taxonomic classes and orders, displaying various relative abundance peaks, with no clear increasing or decreasing trends in the average relative abundance at increasing copper concentrations (not shown here). The taxonomic assignments of all ASVs identified as indicator and non-indicator ASVs can be found in the Supporting Information (Supplementary Table S14).

3.6. Estimating community-level hazard concentration values for a seawater microbiome using a Prokaryotic Sensitivity Distribution

A cumulative probability *Prokaryotic Sensitivity Distribution* (PSD$_{dec}$) was generated for the TITAN-derived change points of decreaser ASVs (Fig. 5A). This allowed the estimation of mHCx$_{dec}$ with 95 % confidence intervals (CI), where the most "sensitive" x percent of decreaser ASVs had reached a TITAN change point. For example, the most sensitive 5 % of ASVs of the Proteobacteria, Verrucomicrobia, and Bacteroidetes phyla were affected at a mHC5$_{dec}$ of 0.61 μg Cu L^{-1} (Fig. 5A&B). See Table 2 for all mHCx values. Since the mHCx$_{dec}$ values were generated from the PSD$_{dec}$ of only decreaser ASVs (a subset of all ASVs in the microbiome) a second PSD$_{all}$ was generated that included all ASVs in the microbiome (including increasers and ASVs with pur.cut/rel.cut <0.95), which amounted to an increase of 63 % in the number of ASV/change points (Supplementary Fig. S6). The mHCx$_{all}$ values derived from the PSD$_{all}$

Table 2
Microbiome Hazard Concentration thresholds (mHCx) for seawater microbiomes exposed to copper based on Bray-Curtis similarities (C-R$_{sim}$; Fig. 2A&B), observed richness (C-R$_{rich}$; Fig. 2C), Shannon diversity (C-R$_{div}$; Fig. 2B) and Prokaryotic Sensitivity Distributions (PSD) generated with change points for amplicon sequence variants (ASVs) identified by Threshold Indicator Taxa ANalysis (TITAN) as decreaser ASVs (PSD$_{dec}$; Fig. 5) or generated with change points of all ASVs included in TITAN (PSDall; Supplementary Fig. S6). mHCx values refer to the copper concentrations at which the microbial community composition, richness or diversity differs from that of the control community by x%, or the concentration at which x% of ASVs reached a TITAN change point (maximum change in relative abundance and/or frequency). Australian Water Quality Guideline Values (WQGVs) are also presented as Protection Concentrations (PC; where e.g., PC95 is comparable to mHC5). All values in μg Cu L^{-1} with 95 % confidence intervals in brackets. NA = not available, – indicates could not be calculated.

mHCx	C-R$_{sim}$	C-R$_{rich}$	C-R$_{div}$	PSD$_{dec}$	PSD$_{all}$	Australian WQGVs
mHC1	0.44 (0.24–2.44)	0.21 (0.20–0.32)	0.24 (0.22–1.85)	0.30 (0.19–0.42)	0.14 (0.11–0.19)	0.3 (PC99)
mHC5	1.05 (0.51–2.61)	0.38 (0.32–0.62)	0.72 (0.50–3.24)	0.61 (0.48–0.81)	0.41 (0.34–0.51)	1.3 (PC95)
mHC10	1.66 (0.88–2.80)	0.80 (0.58–1.40)	2.51 (1.42–6.97)	0.91 (0.74–1.16)	0.74 (0.63–0.88)	3 (PC90)
mHC20	2.69 (1.82–3.41)	3.49 (2.08–6.25)	28.1 (12.0–74.1)	1.49 (1.24–1.83)	1.53 (1.33–1.78)	8 (PC80)
mHC50	8.08 (4.22–13.3)	–	–	4.05 (3.32–4.95)	7.24 (6.06–8.71)	NA

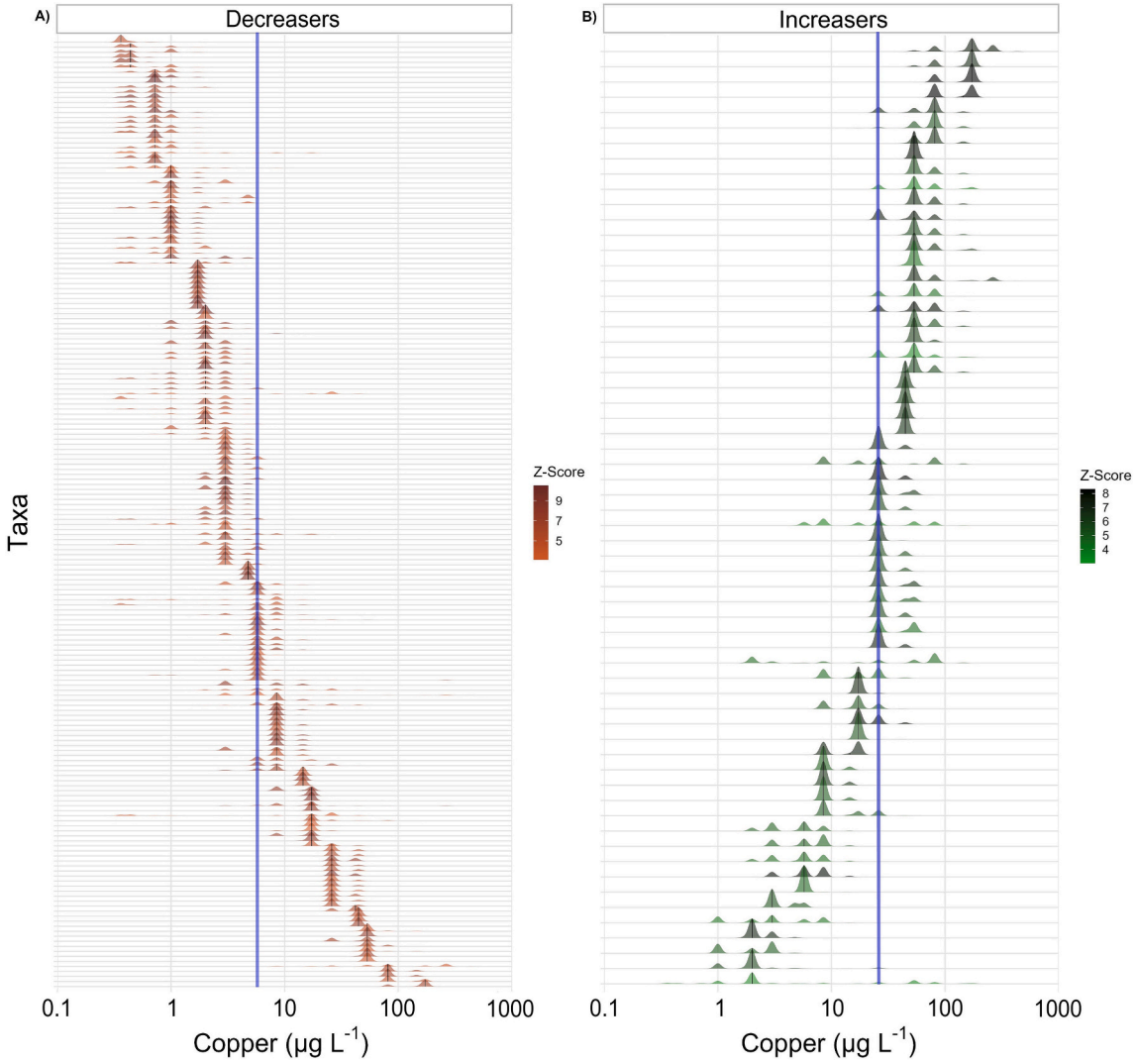

Fig. 3. Indicator taxa identified by Threshold Indicator Taxa ANalysis (TITAN) in the seawater microbiome exposed to 10 copper concentrations. A) Decrease in the relative abundances and/or frequencies of individual amplicon sequence variants (ASVs) (decreasers), B) Increase in the relative abundances and/or frequencies of individual ASVs (increasers). Within each figure, ASV change points (copper concentration resulting in the largest indicator z-scores) are visualized as a probability density function of the bootstrapped replicates (nBoot = 1000) and ranked based on descending order of the 50 % change point quantiles among bootstrap replicates (the central tendency of the probability density function) (Baker et al., 2022). The colour gradients are proportional to the indicator z score (magnitude of change). Only indicator ASVs with purity and reliability scores ≥0.95 that contribute to the overall fsum(z) are shown. Blue lines represent filtered sum(z) community change points for decreasers (fsum(z)- = 5.75 µg Cu L^{-1}) and increasers (fsum(z) + = 17.3 µg Cu L^{-1}). See Supplement Information for individual high-quality figures with ASV identifiers (Supplementary Fig. S4 which can be referred to the taxonomy of the Supplementary Table S14) arranged along the y-axis.

were fairly robust to this modification, mostly overlapping with their respective *m*HCx$_{dec}$ values (Table 2). Notably, the *m*HC50$_{all}$ was nearly two-times greater than the *m*HC50$_{dec}$ (Table 2).

4. Discussion

This study addressed some of the current limitations of deriving ecologically relevant toxicity thresholds and water quality guideline values for marine microbiomes by combining a variety of analytical, toxicity and molecular analysis tools. Our findings, based on comparative relative abundance analyses, suggest that tropical marine microbiomes are particularly sensitive to environmental stress caused by copper contamination and that threshold values established for community composition, richness, diversity, and changes in relative abundance could serve as useful indicator guidelines for copper pollution in coral reef ecosystems. The ecological relevance of the experimentally derived guideline values presented here for marine microbiomes should be further validated by assessing the loss of microbial function and/or activity (e.g. shotgun metagenomics, metatranscriptomics) in the same samples. *Functional* Hazard Concentration values (*f*HCx), ensuring the protection of sensitive yet ecologically important microbial functions, could then be derived from a *Functional Sensitivity Distribution* (FSD), enabling a combined PSD–FSD approach for establishing water quality guideline values in future.

4.1. Response of the seawater microbiome to copper

Exposure to increasing concentrations of copper led to significant shifts in the structure of microbial communities. These changes became more pronounced as the exposure duration increased, particularly in communities treated with propidium monoazide (PMA). While 16S rRNA amplicon gene sequencing provides a robust tool for microbiome research, it remains challenging to distinguish between viable and nonviable microorganisms present in a sample (Nocker et al., 2006). However, this distinction is essential when preforming ecotoxicology testing, where concentration-response modelling should only include

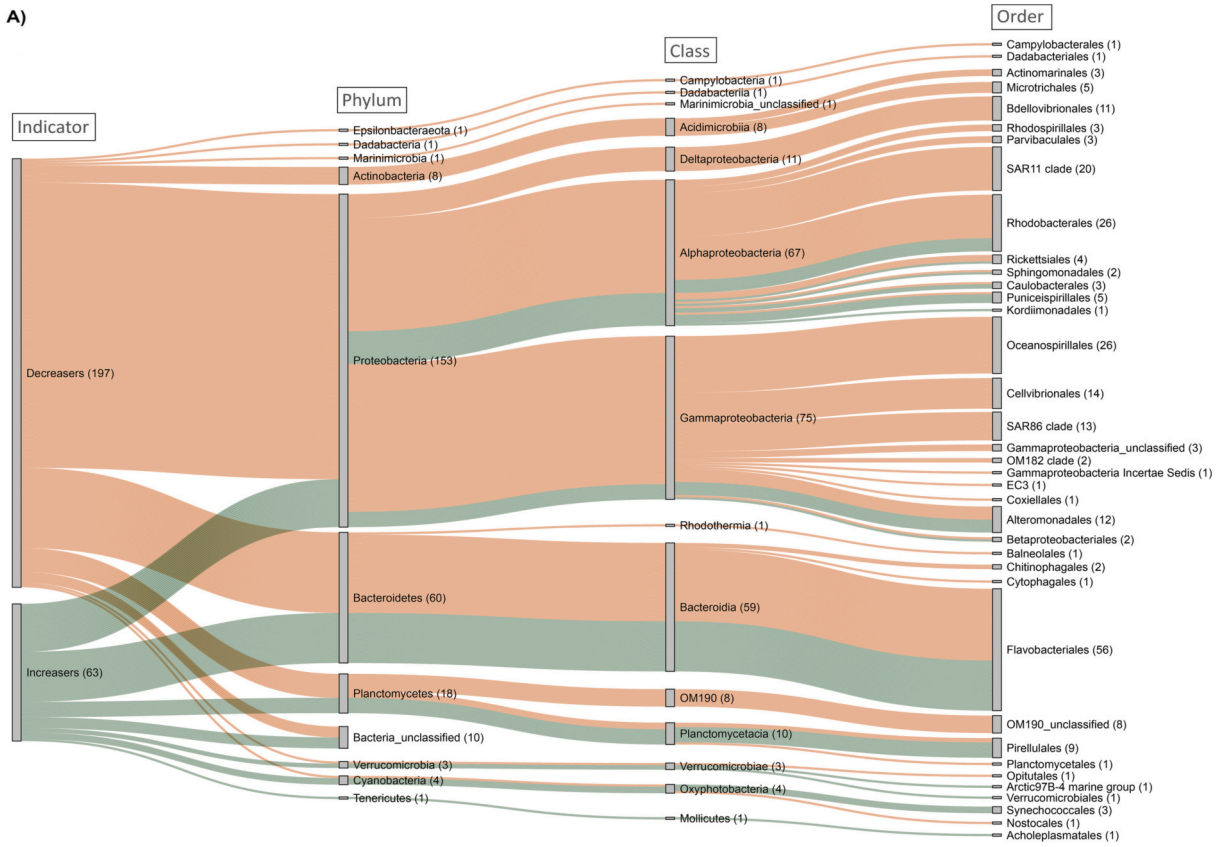

Fig. 4. A) Sankey diagram depicting the taxonomic affiliation of the 260 indicator amplicon sequence variants (ASVs) identified in the Threshold Indicator Taxa ANalysis (TITAN) at indicator, phylum, class, and order level (see Supplementary Table S13 for further taxonomy). B) Scatterplot with smoothed line using the Generalized Additive Model method to visualize changes in the relative abundance (%) of the top 20 most abundant indicator ASVs (assigned at order level and coloured by TITAN indicator response) to increasing copper concentrations ($n = 3$ replicates). Dashed blue line indicates TITAN derived change point of individual ASVs. Responses of all indicator ASVs can be found in the Supporting Information (Supplementary Fig. S5).

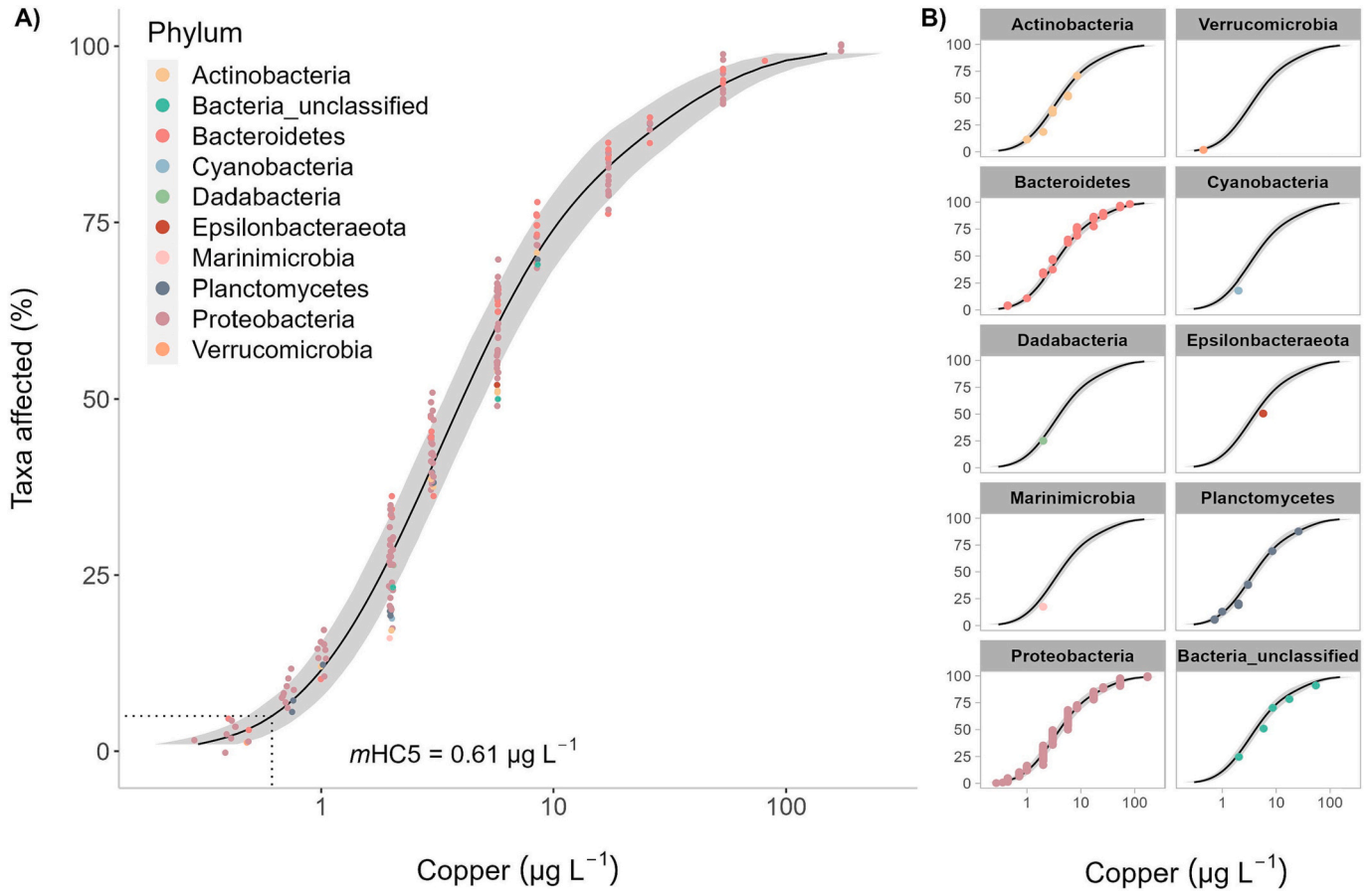

Fig. 5. Cumulative probability *Prokaryotic Sensitivity Distribution* (PSD_{dec}) for dissolved copper in marine water. A) Average fit based on the relative weights of the distributions generated from Threshold Indicator Taxa ANalysis (TITAN) change points of the 197 decreaser amplicon sequence variants (ASVs). The model-averaged 95 % confidence interval is shown by the shaded area and the dotted line represents the model-averaged 5 % *microbiome* Hazard Concentration ($mHC5_{dec}$) of 0.61 µg Cu L^{-1}, where copper is predicted to cause a decrease in the relative abundance and/or frequency (TITAN change points) in the most sensitive 5 % of ASVs (see Table 2 for all *m*HCx values). Data points were jittered for presentation to handle overplotting. B) Individual distribution of ASVs along the averaged fit grouped by phyla. Note all other ASVs unclassified at phylum level were included in estimates as Bacteria_unclassified.

viable community members, akin to a survival assessment for eukaryotic taxa.

The application of PMA resulted in lower DNA yields, suggesting signals from relic DNA were reduced in PMA-treated communities without compromising the proportion of intact cells (since the control microbiomes showed uniform community assembly patterns and no compositional dissimilarities were observed between PMA-treated and PMA-untreated communities). However, compositional differences between communities intensified as copper concentrations increased, with copper exposed communities becoming more rapidly distinct from the control microbiomes. Notably, cells with intact membranes are not automatically assumed to be viable, as intact cells can experience a loss of functionality or metabolic activity before membrane disintegration (Nocker and Camper, 2009).

The effectiveness of PMA has been validated in several studies across various cell or sample types (such as soil, spacecraft cleanrooms, zebrafish, faecal cells in seawater, food samples) (Bae and Wuertz, 2009; Carini et al., 2016; Hirohara et al., 2021; Pan and Breidt Jr, 2007; Vaishampayan et al., 2013). However, PMA performance can be highly influenced by various factors such as microbial community properties (e.g., initial biomass, sample types, and compositional diversity) dye concentration, light exposure, incubation time and temperature, as well as sample turbidity and salt content (Emerson et al., 2017; Wang et al., 2021). While some of these factors may have influenced the current study, the sample type, biomass, initial community structure and experimental conditions were all consistent between samples, reducing the likelihood that the efficacy of PMA treatment would differ within the experiment. Despite these limitations, PMA application appears to have potential to reduce DNA signals of membrane-compromised cells from the analysis in controlled contaminant exposure experiments, but the effectiveness of this technique should be further assessed with natural seawater samples and against other methods, such as cell-viability flow cytometry, cellular metabolism (e.g. stable isotope labelling), RNA-based methods (e.g. transcriptomics) or protein-based methods (e.g. proteomics).

4.2. *Concentration-response relationships for community structure and diversity*

Traditional multivariate analysis methods (i.e. cluster analysis, principal component analysis, correspondence analysis, multidimensional scaling, network analysis) and hypothesis-driven techniques (e.g., permutational multivariate analysis of variance, redundancy analysis, Mantel tests) represent powerful tools to study microbial community assembly patterns (Galloway-Peña and Hanson, 2020; Ramette, 2007). However, these applications have limited efficiency to estimate effect thresholds or identify response profiles of individual taxa. Quantitative methods, such as concentration-response modelling are not typically used for microbial community analysis but could be more suitable in identifying relevant risk thresholds. By applying multi-model fitting with Bayesian model averaging, we demonstrated that microbial community composition, diversity, and richness were substantially reduced

in response to copper exposure. Threshold values were estimated at concentrations of $m\text{HC}_{\text{sim}} = 1.05$ (Fig. 2B), $m\text{HC}_{\text{div}} = 0.72$ μg Cu L^{-1} (Fig. 2C), and $m\text{HC}_{\text{rich}} = 0.38$ (Fig. 2C), respectively, indicating marine microbiomes can already be impaired by low concentrations of copper. Notably, the $m\text{HC1}_{\text{rich}}$ to $m\text{HC10}_{\text{rich}}$ estimates were substantially lower than the respective $m\text{HCx}_{\text{sim}}$ and $m\text{HCx}_{\text{div}}$ thresholds, driven by two low ASV richness values at 0.27 μg Cu L^{-1}. Diversity measures (e.g., Shannon index, richness, evenness) are often influenced by systemic biases introduced in sequence-based microbiome studies, such as DNA extraction, library preparation and sequencing (e.g., PCR amplification, primer choice, sequencing depths), as well as downstream bioinformatic analysis (e.g., pre-filtering, rarefaction) (Nearing et al., 2021). Since both sample richness and sample-based richness estimators are highly sensitive to sampling effort and relative abundance, their estimation is strongly influenced by the detection of rare taxa (Roswell et al., 2021). This could result in an increased estimation uncertainty, emphasizing the need for exercising caution when assessing guideline values based on richness estimators. Nevertheless, the derived thresholds for copper are similar to concentration ranges typically reported in moderately to highly contaminated tropical marine environments (Bakary et al., 2015; Jonathan et al., 2011; Kroon et al., 2015; Stauber and Davies, 2000).

Thresholds generated from concentration-response relationships based on microbial diversity and community (dis)similarities have been proposed before by Arbel et al. (2015), where a Bayesian nonparametric model was applied to assess the response of Antarctic soil microbial communities to fuel contamination. Toxicity thresholds for copper have not been previously reported for marine microbiomes, but it has been demonstrated copper can elicit ecotoxicological effects on microbial communities found in other marine ecosystems or host species, such as biofilms (Corcoll et al., 2019), sediments (Yang et al., 2018), soil (Kou et al., 2018), corals (Gissi et al., 2019), and sponges (Webster et al., 2001). For example, copper affected diversity and community structure of marine periphytic biofilms collected on the west coast of Sweden at 3.81 μg Cu L^{-1} (Corcoll et al., 2019), and shifted the microbiomes of the coral *Acropora muricata* and the sponge *Rhopaloeides odorabile* at 11 μg Cu L^{-1} (Gissi et al., 2019) and 19.4 μg Cu L^{-1} (Webster et al., 2001), respectively. Although, direct comparisons between studies should be drawn with caution (due to differences in microbial species and ecosystem types, for example host tissue may moderate or exacerbate the exposure of symbiotic microbiomes to contaminants such as copper), toxicity thresholds for marine microbial communities estimated in this study are substantially lower than those reported in other studies.

Ecotoxicology studies predominantly assess the response of a single species, but contamination often has broader implications for entire aquatic communities and ecosystems. While potentially introducing some experimental artefacts, microcosm exposures, similar to the system applied here, allow for ecological competition and taxa substitution to shape the communities under acute and chronic toxicant exposure, resembling in situ conditions more closely than toxicity tests on single species. The rapid turnover of marine microorganisms ensures that over a short exposure period, the community-level response to a toxicant captures a mixed combination of survival, growth, and reproduction responses of individual taxa within the community. These responses are dynamically influenced by intricate interactions that change with a shifting community structure and the increase of dissolved organic carbon (DOC) at higher contaminant concentrations, originating from various processes such as the decomposition of organic matter (e.g., rare taxa might exhibit an increased susceptibility to copper, resulting in their accelerated decline). As a primary carbon and energy source, an increased availability of DOC may contribute to an enhanced microbial activity of taxa that respond positively to copper. This hormetic or subsidy-stress response could potentially drive a phase shift within the system towards a distinct community state characterized by a dissimilar community structure and functional potential compared to the original community state. The resultant secondary changes in water chemistry can further influence the toxicity of copper, for example, the aquatic toxicity of copper is expected to reduce with increasing DOC concentrations (ANZG, 2018, 2023) due to the formation of soluble complexes that reduce the availability of free copper ions (Brooks and Waldock, 2009). This complexation reduces the toxicity of copper to aquatic life, which may explain the observed increase in community composition similarity, diversity, and richness at copper concentrations >100 μg L^{-1}. These responses and their collective outcome represent a practical and valuable metric for understanding the impact of contaminants on the microbial ecosystem as a whole and are ecologically relevant in situ. In this context, we propose the use of *m*HCx values for deriving microbial community thresholds, rather than effect concentration values (ECx), which represent a measure of an x% decline in a single toxicity endpoint for a single species.

4.3. Identification of microbial indicator taxa using TITAN

TITAN has found wide application in community ecology to explain taxon contributions to community changes along environmental gradients in diverse environments (e.g. aquatic, sediment, soil) and for various environmental, climate and geographical variable gradients (Gieswein et al., 2019; Jiao and Lu, 2020; Simonin et al., 2019; van der Linde et al., 2018). In this study, TITAN identified 37 % of microbial indicator ASVs that exhibited a statistically reliable response to copper, with a substantially larger proportion responding with a decrease in relative abundance and/or frequency to copper. Taxon change points for decreasers were also observed at lower concentrations than those of increasers. The copper concentration at which the greatest synchronous decline in the relative abundances and/or frequencies of ASVs (fsum(z-)) was estimated to be 5.75 μg Cu L^{-1}. The fsum(z-) does not represent the lowest threshold at which the most sensitive ASVs are affected, rather it signifies the copper concentration at which the greatest aggregate of community change occurs (Baker and King, 2010). The fsum(z-) value therefore is not directly comparable to lower thresholds identified for community composition (using concentration-response modelling); however, it was similar to the concentration at which the community similarity was half of that in the control treatment ($m\text{HC50}_{\text{sim}} = 8.08$ μg Cu L^{-1}). Despite the significant shift in community composition, TITAN analysis identified the majority of taxa (63 %) as non-indicators (purity and reliability scores <0.95). This could be attributed to the stringent data requirements by TITAN to identify statistically reliable indicator taxa via bootstrapping. For example, non-indicator taxa could include taxa with an inconsistent response pattern, as well as taxa present in only a limited number of samples or at relatively low abundance, making them unable to be confidently identified as robust responders despite exhibiting an increasing or decreasing response pattern. Extending the copper concentration gradient (increasing the number of concentrations), while reducing sample replication when applying TITAN, is likely to improve the ability of TITAN to detect reliable indicator taxa through bootstrapping. In studies of this nature, TITAN could prove valuable as a screening tool for identifying indicator taxa for the generation of individual concentration-response curves (e.g., using Bayesian concentration-response model averaging).

4.4. Comparison of relative taxon-specific changes

TITAN analysis revealed that indicator taxa were broadly phylogenetically distributed and consistent taxa responses were only observed within a few specific taxonomic groups. These results are likely due to copper's nonspecific toxicity that can impact multiple processes including the cellular redox potential (formation of reactive oxygen species), protein function (due to copper displacing other metals from binding sites), damage of nucleic acids as well as result in protein misfolding or inhibition of essential processes, like lipoprotein and peptidoglycan maturation (Giachino and Waldron, 2020). The potential for copper to elicit different responses within a taxonomic group, indicates that attempts to apply community-based toxicity thresholds at higher

taxonomic ranks (e.g., phylum, class, order or family level) is likely to be confounded by opposing responses by closely related taxa, emphasizing the importance of establishing threshold values at the ASV-level in future studies.

Generally, there is limited knowledge of the response of tropical marine microbiomes to copper, indeed most of our understanding of copper toxicity on prokaryotes stems from research conducted on the bacterial model organism *Escherichia coli* (Dupont et al., 2011; Giachino and Waldron, 2020; Outten et al., 2000). Several studies support the hypothesis that prokaryotes have evolved a range of taxa-specific mechanisms allowing them to maintain copper homeostasis, while controlling intracellular copper to avoid cellular toxicity (Rensing and McDevitt, 2013; Ridge et al., 2008). These mechanisms include the involvement of transmembrane copper export proteins, copper sequestration by metallothioneins, and copper detoxification (Ladomersky and Petris, 2015). For example, while metallothioneins are commonly found in eukaryotes, they are comparatively rare in bacteria, but have been identified in the cyanobacterium *Synechococcus* sp. (Olafson et al., 1979). In this study, taxa belonging to the order Synechococcales were exclusively identified as increasing indicators and these results are consistent with previous studies where *Synechococcus* was reported to be relatively copper resistant across a range of environments in the Sargasso Sea (Mann et al., 2002). Moreover, the distribution and abundance of marine cyanobacteria is significantly influenced by the metal bioavailability of copper, as these organisms have a high copper requirement for the photosynthetic electron transfer protein, plastocyanin (Huertas et al., 2014; Mann et al., 2002).

This highlights the challenge posed by extending single-species toxicology testing to the community level. Typically, ecotoxicology assessments are conducted using species that exhibit a strict monotonic declining response to a specific stressor. Yet, when applying this approach to establish thresholds on a microbial community scale, we encounter a substantial portion of taxa that respond with a hormetic concentration response, characterized by a dose-stimulation. While quantitative modelling of non-montonic response curves is a key step in understanding its impact and implication at the whole ecosystem scale (Zhu et al., 2013), these types of response patterns receive less consideration in the generation of Species Sensitivity Distributions (SSDs). In this context, deviating from the traditional SSD approach based solely on effect concentration thresholds causing a decline is essential. This transition requires acknowledging that alterations in a community, irrespective of response type, drive the community towards a distinct state, characterized by a dissimilar community structure and function potential compared to the original community state.

4.5. Deriving water quality guideline values for a seawater microbiome

The generation of a copper exposure PSD_{dec} for a tropical marine seawater microbiome derived from TITAN change points enabled the estimation of *m*HCx values based on a single chronic exposure experiment. Here, the $mHC5_{dec}$ represents a concentration below which 95 % of the decreasing indicator community would be protected from copper exposure. This approach is similar to that used to derive water quality guideline values in Australia, where PC95 values (equivalent to HC5) are estimated from SSDs (Warne et al., 2018). The current Australian guideline values for copper have been generated from SSDs that include primarily eukaryotic toxicity data (i.e., 70 marine species from five taxonomic groups) (ANZG, 2018). However, similar datasets are not available for the response of marine microbial communities to contaminants, such as copper, and only two studies have applied the SSD methodology to microbial communities. Doolette et al. (2016) derived the first SSD for prokaryotes based on the response of soil microbial communities to silver contamination, while Yang et al. (2018) later developed a microbial SSD for copper-contaminated sediment communities (field and laboratory cultured communities). In this study, the $mHC5_{dec}$ guideline values of copper based on 197 microbial taxa representing 10 phyla was estimated as 0.61 μg Cu L^{-1}, over two-fold lower than the marine Australian and New Zealand default HC5 of 1.3 μg Cu L^{-1} based on eukaryotic data (ANZG, 2018). However, the $mHC1_{dec}$ and $mHC5_{dec}$ values were lower than the limit of reporting for copper in seawater of 0.7 μg L^{-1}, introducing a degree of uncertainty as the lower three copper concentrations (including the control concentration of 0.18 μg L^{-1}) were estimated from a regression analysis. This is a common issue for toxicity studies, where low effect concentrations are similar to the analytical resolution and ultra-trace copper analysis may help resolve the accuracy of ambient copper concentration measurements in future investigations. Nevertheless, the derived control concentration was consistent with dissolved copper concentrations of 0.09 to 0.3 μg L^{-1} for uncontaminated coastal waters, including the Great Barrier Reef (Apte et al., 2017; Kroon et al., 2015; Stauber and Davies, 2000). Further studies applying improved analytical resolution along with quantitative microbiome profiling are needed for validation of the estimated *m*HCx values for copper-exposed marine microbiomes.

Our findings suggest that marine microbial communities may be more sensitive to copper than eukaryotic taxa, and that the current marine copper guideline values may not be sufficiently protective for these communities. For example, some microbial taxa such as those belonging to Proteobacteria, Verrucomicrobia, and Bacteroidetes phyla displayed a greater sensitivity to copper than most macroinvertebrates (change points less than the ANZG HC1 (PC99) of 0.3 μg Cu L^{-1}). While the established water quality guideline values may not sufficiently safeguard the community structure, further research is warranted to examine the effects of copper toxicity at the functional level within the same community. This is particularly important as alterations in community structure may not directly correspond to modifications in the functional potential of the community due to the functional redundancy inherent in most microbial ecosystem (Allison and Martiny, 2008; Louca et al., 2018; Yin et al., 2000). However, even if certain community members retain the capacity to perform analogous functions akin to the original community, the overall decline in microbial cell abundance with increasing copper exposure could ultimately result in the reduced efficiency and/or generation of the same metabolic by-products, and eventually (directly or indirectly) influence the metabolic activity of the entire community (Riah-Anglet et al., 2015).

To our knowledge, this is the first study to construct a cumulative distribution of effect responses with DNA sequence data for marine microbiomes exposed to copper. Although, PSDs and SSDs are both represent cumulative distributions of taxa sensitivity against a contaminant concentration, there are some differences that should be noted when making direct comparisons. SSDs are generated from EC10, NOEC (No Observed Effect Concentration) or NEC (No Effect Concentration) data which represent low but quantitatively meaningful or significant thresholds at (or below) which toxicity was not observed (Duboudin et al., 2004; Warne et al., 2018). The TITAN change points used to generate the PSD_{dec} also represent statistically meaningful concentrations, but differ in that individual change points are related to the magnitude of change in relative abundance and/or frequency along the copper concentrations (indicated by z-scores) (Baker and King, 2010). In some cases, change point values may be numerically similar to EC10s (if the maximum change is small), while others may be more similar to EC50 values (where maximum change is large, see examples in Fig. 4B). In this sense, the estimated change points do not represent a uniform effect threshold metric, but instead reflect the most reliable estimation of response concentrations. $mHCx_{dec}$ values derived from the PSD_{dec} approach may therefore result in less conservative (higher) thresholds than guideline values estimated from a traditional SSD approach. Furthermore, the applied copper treatments do not represent a series of unique concentrations along a gradient (as normally addressed by TITAN), but rather a discrete series of concentrations with replication. In this instance, the generated change points are often restricted to the applied treatment concentrations and therefore resemble a No Observed Effect Concentration (NOEC) which is the

highest tested concentration, where no statistically significant difference of effect is observed relative to the control. However, it should be emphasized that the *m*HCx$_{dec}$ values were derived from a modelled distribution of TITAN change points and are therefore not constrained to the applied treatment values. The *m*HCx$_{dec}$ values estimated from change points of ASVs that decreased in relative abundance were similar to the *m*HCx$_{all}$ values derived from change points of all ASVs included in the TITAN analysis. For instance, the 5th percentile of most sensitive decreasing ASVs were affected at a *m*HC5$_{dec}$ of 0.61 μg Cu L^{-1}, comparable to the PSD$_{all}$ *m*HC5 of 0.41 μg Cu L^{-1}, representing the concentration at which 5 % of all ASVs in the microbiome underwent maximum change in relative abundance/and or frequency. Although this later approach included change points of ASVs with purity and reliability values below 0.95, as well as ASVs identified by TITAN as increasers, the agreement between the *m*HCx values obtained from both PSD approaches provides evidence that the *m*HC5$_{dec}$ of copper-sensitive decreasing ASVs is representative of relative changes across the entire microbiome.

4.6. Outlook for deriving microbial toxicity thresholds

This study provides a holistic (modelling) approach for establishing ecologically relevant toxicity thresholds for marine microbiomes at both community- and ASV-level. This approach will have broad utility for microbial systems associated with a diversity of habitats, yet there are several limitations that need to be considered in applying toxicity thresholds and guideline values derived in this way. For example, DNA metabarcoding of microbiome data generally provides information on the proportional representation of different taxa within a community but does not reveal the absolute taxa abundance (Vandeputte et al., 2017). By incorporating absolute quantification of microbial abundances encompassing both cell-based (e.g., flow cytometry) and molecular methods (e.g., qPCR, dPCR, ddPCR), quantitative microbiome profiling has the potential to validate the established metabarcoding approach but also highlights any potential limitations in deriving thresholds based on relative abundance data. This would facilitate absolute concentration-response modelling of individual taxa within the community and represents an important future development in microbial ecotoxicology towards a quantitative diagnosis.

Adding to the challenge of interpreting ecological relevance, microbial responses to contaminants assessed via community profiling do not address changes in key functions or metabolic pathways. This holds significant importance as it seems that certain metabolic functions might be decoupled from the taxonomic community composition or phylogeny, potentially due to the adaptive loss of function, convergent evolution, and horizontal gene transfer (Louca et al., 2018). Moreover, most metabolic functions are not monophyletic, meaning no single species exclusively represents a specific function (Martiny et al., 2015). As such, measuring the taxa abundances by a phylogenetic marker is not necessarily indicative of the functional characteristics. This will require the incorporation of multi-omics sequencing approaches, such as shotgun metagenomics, metatranscriptomics, and metabolomics allowing for inference of functional and metabolic capabilities in parallel to abundance profiling (Bashiardes et al., 2016; Hugenholtz and Tyson, 2008). For example, Webster et al. (2018) proposed addressing this issue with a combination of metagenomic/metatranscriptomic sequencing and stable isotope analysis methods to differentiate active from nonactive cells. Concentration-response curves for individual microbial functions could augment taxa-based approaches developed here, with the generation of *Functional Sensitivity Distributions* (FSDs) allowing the estimation of Hazard Concentrations for microbial community functions (i.e., *f*HCx). Challenges include our incomplete understanding of interaction networks, functional redundancy, and the potential for missing/undiscovered microbial functions.

When deriving water quality guideline values at microbial scales one must also consider that estimates of microbial taxa sensitivities may vary substantially for communities of different source environments, due to environmental variation, spatial heterogeneity and niche partitioning (Frade et al., 2020; Muscarella et al., 2019). Thus, it may not be feasible to develop universal guidelines that apply equally to a wide range of microbial communities found in tropical marine ecosystems. A framework that accounts for site-specific risk thresholds is therefore needed for developing tailored water quality guideline values that can be refined and adapted according to local environmental conditions and site disturbance history (van Dam et al., 2019). Comparisons of microbial community responses across locations could also aid in characterizing core microbiomes or indicator microorganisms that are consistently sensitive to a particular stressor or multiple stressors across diverse human-impacted environments (Abreu et al., 2022).

5. Conclusion

Building a comprehensive baseline dataset of response profiles and thresholds for microbiomes across habitats is critical to developing a global understanding of how prokaryotes respond to environmental stress. The methods developed here to derive community level thresholds and Hazard Concentrations for copper contamination by combining 16S rRNA gene amplicon sequencing (restricted to viable cells) with concentration-response modelling and the generation of a cumulative response distribution (based on indicator taxa) represents substantial progress in unifying methods applied in environmental microbiology and ecotoxicology. The *microbiome* Hazard Concentrations derived for copper were lower than the current Australian Water Quality Guideline Value based on eukaryotic communities, suggesting marine microbial communities may be more vulnerable and therefore insufficiently protected from copper pollution. Ultimately, the development of more robust guideline values for microbial communities and/or incorporation of response thresholds for microbial communities into the derivation of guideline values across a broader taxonomic range (combining prokaryotic and eukaryotic threshold data) would represent a major step towards accounting for whole ecosystem responses to anthropogenic pressures.

Supplementary data to this article can be found online at https://doi.org/10.1016/j.scitotenv.2023.166658.

Funding sources

This work was supported by the Australian Research Council under the project DP200100790: Quantifying the impacts of environmental stress on marine microorganisms, the Australian Institute of Marine Science, the Australian Government Research Training Program Fee Offset and Scholarship program from the University of Queensland (Australia).

CRediT authorship contribution statement

Marie C. Thomas: Conceptualization, Methodology, Investigation, Formal analysis, Data curation, Visualization, Writing – original draft, Writing – review & editing. **Gretel Waugh:** Conceptualization, Methodology, Investigation, Writing – review & editing. **Inka Vanwonterghem:** Conceptualization, Methodology, Writing – review & editing. **Nicole S. Webster:** Conceptualization, Methodology, Funding acquisition, Writing – review & editing. **Christian Rinke:** Writing – review & editing. **Rebecca Fisher:** Formal analysis, Writing – review & editing. **Heidi M. Luter:** Conceptualization, Methodology, Investigation, Supervision, Writing – review & editing. **Andrew P. Negri:** Conceptualization, Methodology, Investigation, Supervision, Writing – review & editing.

Declaration of competing interest

The authors declare that they have no known competing financial interests or personal relationships that could have appeared to influence the work reported in this paper.

Data availability

Data will be made available on request.

Acknowledgments

The authors would like to thank the financial sponsors who made this work possible: Australian Research Council (ARC) Discovery Project (DP200100790); support for M.C.T from the University of Queensland, School of Chemistry and Molecular Biosciences and the Australian Centre for Ecogenomics in Brisbane (Australia) and the Australian Institute of Marine Science (AIMS Townsville and Perth, Australia). We extend our gratitude to the staff at AIMS for their expertise, and in particular, Florita Flores, Sara Bell, and Carlos Alvarez-Roa for their time and assistance in performing the experiment. Finally, the authors would like to acknowledge the traditional owners and custodians of the land on which this work was conducted, the Wulgurukaba and Bindal people.

References

Abreu, A., Bourgois, E., Gristwood, A., Troublé, R., Acinas, S.G., Bork, P., Boss, E., Bowler, C., Budinich, M., Chaffron, S., de Vargas, C., Delmont, T.O., Eveillard, D., Guidi, L., Iudicone, D., Kandels, S., Morlon, H., Lombard, F., Pepperkok, R., Karlusich, J.J.P., Piganeau, G., Régimbeau, A., Sommeria-Klein, G., Stemmann, L., Sullivan, M.B., Sunagawa, S., Wincker, P., Zablocki, O., Arendt, D., Bilic, J., Finn, R., Heard, E., Rouse, B., Vamathevan, J., Casotti, R., Cancio, I., Cunliffe, M., Kervella, A. E., Kooistra, W.H.C.F., Obst, M., Pade, N., Power, D.M., Santi, I., Tsagaraki, T.M., Vanaverbeke, J., Tara Ocean, F., Tara, O., European Molecular Biology, L, European Marine Biological Resource Centre - European Research Infrastructure, C, 2022. Priorities for ocean microbiome research. Nat. Microbiol. 7 (7), 937–947. https://doi.org/10.1038/s41564-022-01145-5.

Ainsworth, T.D., Thurber, R.V., Gates, R.D., 2010. The future of coral reefs: a microbial perspective. Trends Ecol. Evol. 25 (4), 233–240. https://doi.org/10.1016/j.tree.2009.11.001.

Allaire, J., Ellis, P., Gandrud, C., Kuo, K., Lewis, B., Owen, J., Russell, K., Rogers, J., Sese, C., & Yetman, C. (2017). Package 'networkD3'. D3 JavaScript network graphs from R. in https://CRAN.R-project.org/package=networkD3.

Allison, S.D., Martiny, J.B., 2008. Resistance, resilience, and redundancy in microbial communities. Proc. Natl. Acad. Sci. 105, 11512–11519. https://doi.org/10.1073/pnas.0801925105.

ANZG, 2018. Revised Australian and New Zealand guidelines for fresh and marine water quality. In: Australian and New Zealand Environment and Conservation Council and Agriculture and Resource Management Council of Australia and new Zealand. Canberra, Australia. https://www.waterquality.gov.au/anz-guidelines/guideline-values/default/water-quality-toxicants/toxicants (accessed 24 April 2023).

ANZG, 2023. Toxicant default guideline values for aquatic ecosystem protection: Dissolved copper in marine water. Australian and New Zealand guidelines for fresh and marine water quality. In: CC BY 4.0. Australian and New Zealand Governments and Australian State and Territory Governments. Canberra, ACT, Australia. https://www.waterquality.gov.au/anz-guidelines/guideline-values/default/water-quality-toxicants/toxicants (accessed 30 May 2023).

Apte, S., Vicente-Beckett, V., Andersen, L., Andrewarthe, J., Angel, B., Shearer, D., Simpson, S., Stauber, J., 2017. Contaminant pathways in port Curtis: final report. https://acquire.cqu.edu.au/articles/report/Contaminant_pathways_in_Port_Curtis_final_report/13452704.

Arbel, J., King, C.K., Raymond, B., Winsley, T., Mengersen, K.L., 2015. Application of a Bayesian nonparametric model to derive toxicity estimates based on the response of Antarctic microbial communities to fuel-contaminated soil. Ecology and Evolution 5 (13), 2633–2645. https://doi.org/10.1002/ece3.1493.

Astudillo-García, C., Hermans, S.M., Stevenson, B., Buckley, H.L., Lear, G., 2019. Microbial assemblages and bioindicators as proxies for ecosystem health status: potential and limitations. Appl. Microbiol. Biotechnol. 103, 6407–6421. https://doi.org/10.1007/s00253-019-09963-0.

Bae, S., Wuertz, S., 2009. Rapid decay of host-specific fecal Bacteroidales cells in seawater as measured by quantitative PCR with propidium monoazide. Water Res. 43 (19), 4850–4859. https://doi.org/10.1016/j.watres.2009.06.053.

Bakary, I., Yao, K.M., Etchian, O.A., Soro, M.B., Trokourey, A., Bokra, Y., 2015. Zinc, copper, cadmium, and lead concentrations in water, sediment, and Anadara senilis in a tropical estuary. Environ. Monit. Assess. 187 (12), 762. https://doi.org/10.1007/s10661-015-4976-6.

Baker, M.E., King, R.S., 2010. A new method for detecting and interpreting biodiversity and ecological community thresholds. Methods Ecol. Evol. 1 (1), 25–37. https://doi.org/10.1111/j.2041-210X.2009.00007.x.

Baker, M. E., King, R. S., Kahle, D., & Kahle, M. D. (2022). TITAN2: threshold Indicator taxa analysis. In (version R package 2.4.1) https://rdocumentation.org/packages/TITAN2/versions/2.4.1.

Banihashemi, A., Van Dyke, M., Huck, P., 2012. Long-amplicon propidium monoazide-PCR enumeration assay to detect viable Campylobacter and Salmonella. J. Appl. Microbiol. 113 (4), 863–873. https://doi.org/10.1111/j.1365-2672.2012.05382.x.

Barton, K., & Barton, M. K. (2015). Package 'mumin'. In (version R package v1.47.1) https://rdocumentation.org/packages/MuMIn/versions/1.47.5.

Bashiardes, S., Zilberman-Schapira, G., Elinav, E., 2016. Use of metatranscriptomics in microbiome research. Bioinformatics and Biology Insights 10. BBI. S34610.

Birrer, S.C., Dafforn, K.A., Johnston, E.L., 2017. Microbial community responses to contaminants and the use of molecular techniques. In: Cravo-Laureau, C., Cagnon, C., Lauga, B., Duran, R. (Eds.), Microbial Ecotoxicology. Springer, pp. 165–183. https://doi.org/10.1007/978-3-319-61795-4_8.

Bissett, A., Brown, M.V., Siciliano, S.D., Thrall, P.H., 2013. Microbial community responses to anthropogenically induced environmental change: towards a systems approach. Ecol. Lett. 16, 128–139. https://doi.org/10.1111/ele.12109.

Bokulich, N.A., Kaehler, B.D., Rideout, J.R., Dillon, M., Bolyen, E., Knight, R., Huttley, G. A., Gregory Caporaso, J., 2018. Optimizing taxonomic classification of marker-gene amplicon sequences with QIIME 2's q2-feature-classifier plugin. Microbiome 6 (1), 90. https://doi.org/10.1186/s40168-018-0470-z.

Bolyen, E., Rideout, J.R., Dillon, M.R., Bokulich, N.A., Abnet, C.C., Al-Ghalith, G.A., Alexander, H., Alm, E.J., Arumugam, M., Asnicar, F., Bai, Y., Bisanz, J.E., Bittinger, K., Brejnrod, A., Brislawn, C.J., Brown, C.T., Callahan, B.J., Caraballo-Rodríguez, A.M., Chase, J., Cope, E.K., Da Silva, R., Diener, C., Dorrestein, P.C., Douglas, G.M., Durall, D.M., Duvallet, C., Edwardson, C.F., Ernst, M., Estaki, M., Fouquier, J., Gauglitz, J.M., Gibbons, S.M., Gibson, D.L., Gonzalez, A., Gorlick, K., Guo, J., Hillmann, B., Holmes, S., Holste, H., Huttenhower, C., Huttley, G.A., Janssen, S., Jarmusch, A.K., Jiang, L., Kaehler, B.D., Kang, K.B., Keefe, C.R., Keim, P., Kelley, S.T., Knights, D., Koester, I., Kosciolek, T., Kreps, J., Langille, M.G.I., Lee, J., Ley, R., Liu, Y.-X., Loftfield, E., Lozupone, C., Maher, M., Marotz, C., Martin, B.D., McDonald, D., McIver, L.J., Melnik, A.V., Metcalf, J.L., Morgan, S.C., Morton, J.T., Naimey, A.T., Navas-Molina, J.A., Nothias, L.F., Orchanian, S.B., Pearson, T., Peoples, S.L., Petras, D., Preuss, M.L., Pruesse, E., Rasmussen, L.B., Rivers, A., Robeson, M.S., Rosenthal, P., Segata, N., Shaffer, M., Shiffer, A., Sinha, R., Song, S.J., Spear, J.R., Swafford, A.D., Thompson, L.R., Torres, P.J., Trinh, P., Tripathi, A., Turnbaugh, P.J., Ul-Hasan, S., van der Hooft, J.J.J., Vargas, F., Vázquez-Baeza, Y., Vogtmann, E., von Hippel, M., Walters, W., Wan, Y., Wang, M., Warren, J., Weber, K. C., Williamson, C.H.D., Willis, A.D., Xu, Z.Z., Zaneveld, J.R., Zhang, Y., Zhu, Q., Knight, R., Caporaso, J.G., 2019. Reproducible, interactive, scalable and extensible microbiome data science using QIIME 2. Nat. Biotechnol. 37 (8), 852–857. https://doi.org/10.1038/s41587-019-0209-9.

Bourne, D., Webster, N., 2013. Coral reef bacterial communities. In: The Prokaryotes–Prokaryotic Communities and Ecophysiology, 4, pp. 163–187. https://doi.org/10.1007/978-3-642-30123-0.

Brooks, M.E., Kristensen, K., Van Benthem, K.J., Magnusson, A., Berg, C.W., Nielsen, A., Skaug, H.J., Machler, M., Bolker, B.M., 2017. glmmTMB balances speed and flexibility among packages for zero-inflated generalized linear mixed modeling. The R Journal 9 (2), 378–400. https://doi.org/10.5167/uzh-148918.

Brooks, S., Waldock, M., 2009. The use of copper as a biocide in marine antifouling paints. In: Advances in Marine Antifouling Coatings and Technologies. Elsevier, pp. 492–521.

Brown, M.V., Van De Kamp, J., Ostrowski, M., Seymour, J.R., Ingleton, T., Messer, L.F., Jeffries, T., Siboni, N., Laverock, B., Bibiloni-Isaksson, J., 2018. Systematic, continental scale temporal monitoring of marine pelagic microbiota by the Australian Marine Microbial Biodiversity Initiative. Scientific Data 5 (1), 1–10. https://doi.org/10.1038/sdata.2018.130.

Callahan, B.J., McMurdie, P.J., Rosen, M.J., Han, A.W., Johnson, A.J.A., Holmes, S.P., 2016. DADA2: high-resolution sample inference from Illumina amplicon data. Nat. Methods 13 (7), 581–583. https://doi.org/10.1038/nmeth.3869.

Caquet, T., Lagadic, L., Sheffield, S.R., 2000. Mesocosms in ecotoxicology (1): outdoor aquatic systems. Reviews of Environmental Contamination and Toxicology: Continuation of Residue Reviews 1-38. https://doi.org/10.1007/978-1-4612-1172-3_1.

Carini, P., Marsden, P.J., Leff, J.W., Morgan, E.E., Strickland, M.S., Fierer, N., 2016. Relic DNA is abundant in soil and obscures estimates of soil microbial diversity. Nat. Microbiol. 2 (3), 1–6. https://doi.org/10.1038/nmicrobiol.2016.242.

Cavicchioli, R., Ripple, W.J., Timmis, K.N., Azam, F., Bakken, L.R., Baylis, M., Behrenfeld, M.J., Boetius, A., Boyd, P.W., Classen, A.T., 2019. Scientists' warning to humanity: microorganisms and climate change. Nat. Rev. Microbiol. 17 (9), 569–586. https://doi.org/10.1038/s41579-019-0222-5.

CCME. (2005). *Statistical analysis of the SSD approach for development of Canadian Water Quality Guidelines* (1414). https://ccme.ca/en/resources/water-aquatic-life# (accessed 16 March 2023).

Clarke, K., Gorley, R. (2015). Getting started with PRIMER v7. *PRIMER-E: Plymouth, Plymouth Marine* Laboratory, 20(1). https://www.primer-e.com/our-software/primer-version-7/.

Corcoll, N., Yang, J., Backhaus, T., Zhang, X., Eriksson, K.M., 2019. Copper affects composition and functioning of microbial communities in marine biofilms at environmentally relevant concentrations. Front. Microbiol. 9, 3248. https://doi.org/10.3389/fmicb.2018.03248.

van Dam, R.A., Hogan, A.C., Harford, A.J., Humphrey, C.L., 2019. How specific is site-specific? A review and guidance for selecting and evaluating approaches for deriving

local water quality benchmarks. Integr. Environ. Assess. Manag. 15 (5), 683–702. https://doi.org/10.1002/ieam.4181.
Doolette, C.L., Gupta, V.V., Lu, Y., Payne, J.L., Batstone, D.J., Kirby, J.K., Navarro, D.A., McLaughlin, M.J., 2016. Quantifying the sensitivity of soil microbial communities to silver sulfide nanoparticles using metagenome sequencing. PLoS One 11 (8), e0161979. https://doi.org/10.1371/journal.pone.0161979.
Duboudin, C., Ciffroy, P., Magaud, H., 2004. Acute-to-chronic species sensitivity distribution extrapolation. Environ. Toxicol. Chem. 23 (7), 1774–1785. https://doi.org/10.1002/etc.5620230723.
Dupont, C.L., Grass, G., Rensing, C., 2011. Copper toxicity and the origin of bacterial resistance—new insights and applications. Metallomics 3 (11), 1109–1118. https://doi.org/10.1039/c1mt00107h.
EFSA, 2013. Panel on plant protection products and their residues. Guidance on tiered risk assessment for plant protection products for aquatic organisms in edge-of-field surface waters. EFSA J. 11 (7), 3290. https://doi.org/10.2903/j.efsa.2013.3290.
Emerson, J.B., Adams, R.I., Román, C.M.B., Brooks, B., Coil, D.A., Dahlhausen, K., Ganz, H.H., Hartmann, E.M., Hsu, T., Justice, N.B., 2017. Schrödinger's microbes: tools for distinguishing the living from the dead in microbial ecosystems. Microbiome 5 (1), 1–23. https://doi.org/10.1186/s40168-017-0285-3.
Fisher, R., Barneche, D., Ricardo, G., Fox, D., 2023. Bayesnec: A Bayesian No-Effect-Concentration (NEC) Algorithm. In (Version R package 2.1.0.2). https://open-aims.github.io/bayesnec/.
Fox, D.R., 2010. A Bayesian approach for determining the no effect concentration and hazardous concentration in ecotoxicology. Ecotoxicol. Environ. Saf. 73 (2), 123–131. https://doi.org/10.1016/j.ecoenv.2009.09.012.
Frade, P.R., Glasl, B., Matthews, S.A., Mellin, C., Serrão, E.A., Wolfe, K., Mumby, P.J., Webster, N.S., Bourne, D.G., 2020. Spatial patterns of microbial communities across surface waters of the great barrier reef. Communications Biology 3 (1), 1–14. https://doi.org/10.1038/s42003-020-01166-y.
Galloway-Peña, J., Hanson, B., 2020. Tools for analysis of the microbiome. Dig. Dis. Sci. 65 (3), 674–685. https://doi.org/10.1007/s10620-020-06091-y.
Giachino, A., Waldron, K.J., 2020. Copper tolerance in bacteria requires the activation of multiple accessory pathways. Mol. Microbiol. 114 (3), 377–390. https://doi.org/10.1111/mmi.14522.
Gieswein, A., Hering, D., Lorenz, A.W., 2019. Development and validation of a macroinvertebrate-based biomonitoring tool to assess fine sediment impact in small mountain streams. Sci. Total Environ. 652, 1290–1301. https://doi.org/10.1016/j.scitotenv.2018.10.180.
Gissi, F., Reichelt-Brushett, A.J., Chariton, A.A., Stauber, J.L., Greenfield, P., Humphrey, C., Salmon, M., Stephenson, S.A., Cresswell, T., Jolley, D.F., 2019. The effect of dissolved nickel and copper on the adult coral Acropora muricata and its microbiome. Environ. Pollut. 250, 792–806. https://doi.org/10.1016/j.envpol.2019.04.030.
Glasl, B., Webster, N.S., Bourne, D.G., 2017. Microbial indicators as a diagnostic tool for assessing water quality and climate stress in coral reef ecosystems. Mar. Biol. 164 (4), 91. https://doi.org/10.1007/s00227-017-3097-x.
Glasl, B., Bourne, D.G., Frade, P.R., Webster, N.S., 2018. Establishing microbial baselines to identify indicators of coral reef health. Microbiology Australia 39 (1), 42–46. https://doi.org/10.1071/MA18011.
Glasl, B., Bourne, D.G., Frade, P.R., Thomas, T., Schaffelke, B., Webster, N.S., 2019. Microbial indicators of environmental perturbations in coral reef ecosystems. Microbiome 7 (1), 1–13. https://doi.org/10.1186/s40168-019-0705-7.
Hartig, F. (2022). DHARMa: residual diagnostics for hierarchical (multi-level/mixed) regression models. In (version R package 0.4.6) http://florianhartig.github.io/DHARMa/.
Haynes, D., Johnson, J.E., 2000. Organochlorine, heavy metal and polyaromatic hydrocarbon pollutant concentrations in the great barrier reef (Australia) environment: a review. Mar. Pollut. Bull. 41 (7–12), 267–278. https://doi.org/10.1016/S0025-326X(00)00134-X.
Hazen, T.C., 2020. Lessons from the 2010 Deepwater Horizon Accident in the Gulf of Mexico. Springer. https://doi.org/10.1007/978-3-319-90569-3_31.
He, F., 2011. *E. coli* genomic DNA extraction. Bio-protocol 1 (14), e97. https://doi.org/10.21769/BioProtoc.97.
Hirohara, T., Tsuri, K., Miyagawa, K., Paine, R.T., Yamanaka, H., 2021. The application of PMA (propidium monoazide) to different target sequence lengths of zebrafish eDNA: a new approach aimed toward improving environmental DNA ecology and biological surveillance. Front. Ecol. Evol. 9, 632973 https://doi.org/10.3389/fevo.2021.632973.
Huertas, M.J., López-Maury, L., Giner-Lamia, J., Sánchez-Riego, A.M., Florencio, F.J., 2014. Metals in cyanobacteria: analysis of the copper, nickel, cobalt and arsenic homeostasis mechanisms. Life 4 (4), 865–886. https://doi.org/10.3390/life4040865.
Hugenholtz, P., Tyson, G.W., 2008. Metagenomics. Nature 455 (7212), 481–483.
Jiao, S., Lu, Y., 2020. Soil pH and temperature regulate assembly processes of abundant and rare bacterial communities in agricultural ecosystems. Environ. Microbiol. 22 (3), 1052–1065. https://doi.org/10.1111/1462-2920.14815.
Jonathan, M.P., Roy, P.D., Thangadurai, N., Srinivasalu, S., Rodríguez-Espinosa, P.F., Sarkar, S.K., Lakshumanan, C., Navarrete-López, M., Muñoz-Sevilla, N.P., 2011. Metal concentrations in water and sediments from tourist beaches of Acapulco, Mexico. Marine Pollution Bulletin 62 (4), 845–850. https://doi.org/10.1016/j.marpolbul.2011.02.042.
Kou, S., Vincent, G., Gonzalez, E., Pitre, F.E., Labrecque, M., Brereton, N.J., 2018. The response of a 16S ribosomal RNA gene fragment amplified community to lead, zinc, and copper pollution in a Shanghai field trial. Front. Microbiol. 9, 366. https://doi.org/10.3389/fmicb.2018.00366.
Kroon, F., Berry, K., Brinkman, D., Davis, A., King, O., Kookana, R., Lewis, S., Leusch, F., Makarynskyy, O., & Melvin, S. (2015). Identification, impacts, and prioritisation of emerging contaminants present in the GBR and Torres Strait marine environments. Report to the National Environmental Science Programme. Reef and Rainforest Research Centre Limited, Cairns (138 pp.). http://www.nesptropical.edu.au.
Ladomersky, E., Petris, M.J., 2015. Copper tolerance and virulence in bacteria. Metallomics 7 (6), 957–964. https://doi.org/10.1039/c4mt00327f.
Lane, D., 1991. 16S/23S rRNA sequencing. In: Stackebrandt, E., Goodfellow, M. (Eds.), Nucleic Acid Techniques in Bacterial Systematics. John Wiley and Sons, New York, pp. 115–175. https://books.google.com.au/books?id=89PwAAAAMAAJ.
Lenth, R., Singmann, H., Love, J., Buerkner, P., Herve, M., 2023. Emmeans: Estimated Marginal Means, aka Least-Squares Means. In (Version R package 1.8.4-1). https://CRAN.R-project.org/package=emmeans.
van der Linde, S., Suz, L.M., Orme, C.D.L., Cox, F., Andreae, H., Asi, E., Atkinson, B., Benham, S., Carroll, C., Cools, N., 2018. Environment and host as large-scale controls of ectomycorrhizal fungi. Nature 558 (7709), 243–248. https://doi.org/10.1038/s41586-018-0189-9.
Louca, S., Polz, M.F., Mazel, F., Albright, M.B.N., Huber, J.A., O'Connor, M.I., Ackermann, M., Hahn, A.S., Srivastava, D.S., Crowe, S.A., Doebeli, M., Parfrey, L.W., 2018. Function and functional redundancy in microbial systems. Nature Ecology and Evolution 2 (6), 936–943. https://doi.org/10.1038/s41559-018-0519-1.
Maher, R.L., Epstein, H.E., Vega Thurber, R., 2022. Dynamics of bacterial communities on coral reefs: Implications for conservation. In: van Oppen, M.J.H., Aranda Lastra, M. (Eds.), Coral Reef Conservation and Restoration in the Omics Age. Coral Reefs of the World, vol. 15. Springer, pp. 97–116. https://doi.org/10.1007/978-3-031-07055-6_7.
Mann, E.L., Ahlgren, N., Moffett, J.W., Chisholm, S.W., 2002. Copper toxicity and cyanobacteria ecology in the Sargasso Sea. Limnol. Oceanogr. 47 (4), 976–988. https://doi.org/10.4319/lo.2002.47.4.0976.
Martin, M., 2011. Cutadapt removes adapter sequences from high-throughput sequencing reads. EMBnet. journal 17 (1), 10–12. https://doi.org/10.14806/EJ.17.1.200.
Martiny, J.B., Jones, S.E., Lennon, J.T., Martiny, A.C., 2015. Microbiomes in light of traits: a phylogenetic perspective. Science 350 (6261), aac9323. https://doi.org/10.1126/science.aac9323.
McDevitt-Irwin, J.M., Baum, J.K., Garren, M., Vega Thurber, R.L., 2017. Responses of coral-associated bacterial communities to local and global stressors. Front. Mar. Sci. 262 https://doi.org/10.3389/fmars.2017.00262.
McMurdie, P.J., Holmes, S., 2013. Phyloseq: an R package for reproducible interactive analysis and graphics of microbiome census data. PLoS One 8 (4), e61217. https://doi.org/10.1371/journal.pone.0061217.
Muscarella, M.E., Boot, C.M., Broeckling, C.D., Lennon, J.T., 2019. Resource heterogeneity structures aquatic bacterial communities. The ISME Journal 13 (9), 2183–2195. https://doi.org/10.1038/s41396-019-0427-7.
Nearing, J.T., Comeau, A.M., Langille, M.G., 2021. Identifying biases and their potential solutions in human microbiome studies. Microbiome 9 (1), 1–22. https://doi.org/10.1186/s40168-021-01059-0.
Nocker, A., Camper, A.K., 2009. Novel approaches toward preferential detection of viable cells using nucleic acid amplification techniques. FEMS Microbiol. Lett. 291 (2), 137–142. https://doi.org/10.1111/j.1574-6968.2008.01429.x.
Nocker, A., Cheung, C.-Y., Camper, A.K., 2006. Comparison of propidium monoazide with ethidium monoazide for differentiation of live vs. dead bacteria by selective removal of DNA from dead cells. J. Microbiol. Methods 67 (2), 310–320. https://doi.org/10.4018/978-1-60566-840-6.ch008.
Nocker, A., Sossa-Fernandez, P., Burr, M.D., Camper, A.K., 2007. Use of propidium monoazide for live/dead distinction in microbial ecology. Appl. Environ. Microbiol. 73 (16), 5111–5117. https://doi.org/10.1128/aem.02987-06.
Nogales, B., Lanfranconi, M.P., Piña-Villalonga, J.M., Bosch, R., 2011. Anthropogenic perturbations in marine microbial communities. FEMS Microbiol. Rev. 35 (2), 275–298. https://doi.org/10.1111/j.1574-6976.2010.00248.x.
Olafson, R., Abel, K., Sim, R., 1979. Prokaryotic metallothionein: preliminary characterization of a blue-green alga heavy metal-binding protein. Biochem. Biophys. Res. Commun. 89 (1), 36–43. https://doi.org/10.1016/0006-291X(79)90939-2.
Outten, F.W., Outten, C.E., Hale, J., O'Halloran, T.V., 2000. Transcriptional activation of an Escherichia coliCopper efflux regulon by the chromosomal MerR homologue, CueR. Journal of Biological Chemistry 275 (40), 31024–31029. https://doi.org/10.1074/jbc.M006508200.
Pan, Y., Breidt Jr., F., 2007. Enumeration of viable listeria monocytogenes cells by real-time PCR with propidium monoazide and ethidium monoazide in the presence of dead cells. Appl. Environ. Microbiol. 73 (24), 8028–8031. https://doi.org/10.1128/aem.01198-07.
Pedregosa, F., Varoquaux, G., Gramfort, A., Michel, V., Thirion, B., Grisel, O., Blondel, M., Prettenhofer, P., Weiss, R., Dubourg, V., 2011. Scikit-learn: machine learning in Python. *The*. J. Mach. Learn. Res. 12, 2825–2830. http://scikit-learn.sourceforge.net.
Posthuma, L., van Gils, J., Zijp, M.C., van de Meent, D., de Zwart, D., 2019. Species sensitivity distributions for use in environmental protection, assessment, and management of aquatic ecosystems for 12 386 chemicals. Environ. Toxicol. Chem. 38 (4), 905–917. https://doi.org/10.1002/etc.4373.
Quast, C., Pruesse, E., Yilmaz, P., Gerken, J., Schweer, T., Yarza, P., Peplies, J., Glöckner, F.O., 2012. The SILVA ribosomal RNA gene database project: improved data processing and web-based tools. Nucleic Acids Res. 41 (D1), D590–D596. https://doi.org/10.1093/nar/gks1219.
R Core Development Team. (2023). R: A language and environment for statistical computing. In R Foundation for Statistical Computing. https://www.R-project.org/.

Ramette, A., 2007. Multivariate analyses in microbial ecology. FEMS Microbiol. Ecol. 62 (2), 142–160. https://doi.org/10.1111/j.1574-6941.2007.00375.x.
Rensing, C., McDevitt, S.F., 2013. The copper metallome in prokaryotic cells. Metallomics and the Cell 417–450. https://doi.org/10.1007/978-94-007-5561-1_12.
Riah-Anglet, W., Trinsoutrot-Gattin, I., Martin-Laurent, F., Laroche-Ajzenberg, E., Norini, M.-P., Latour, X., Laval, K., 2015. Soil microbial community structure and function relationships: a heat stress experiment. Appl. Soil Ecol. 86, 121–130. https://doi.org/10.1016/J.APSOIL.2014.10.001.
Ridge, P.G., Zhang, Y., Gladyshev, V.N., 2008. Comparative genomic analyses of copper transporters and cuproproteomes reveal evolutionary dynamics of copper utilization and its link to oxygen. PLoS One 3 (1), e1378. https://doi.org/10.1371/journal.pone.0001378.
Roswell, M., Dushoff, J., Winfree, R., 2021. A conceptual guide to measuring species diversity. Oikos 130 (3), 321–338.
Salam, K.W., El-Fadel, M., Barbour, E.K., Saikaly, P.E., 2014. A propidium monoazide–quantitative PCR method for the detection and quantification of viable enterococcus faecalis in large-volume samples of marine waters. Appl. Microbiol. Biotechnol. 98 (20), 8707–8718. https://doi.org/10.1007/s00253-014-6023-x.
Shahsavari, E., Aburto-Medina, A., Khudur, L.S., Taha, M., Ball, A.S., 2017. From microbial ecology to microbial ecotoxicology. In: Microbial Ecotoxicology. Springer, pp. 17–38. https://doi.org/10.1007/978-3-319-61795-4_2.
Simonin, M., Voss, K.A., Hassett, B.A., Rocca, J.D., Wang, S.Y., Bier, R.L., Violin, C.R., Wright, J.P., Bernhardt, E.S., 2019. In search of microbial indicator taxa: shifts in stream bacterial communities along an urbanization gradient. Environ. Microbiol. 21 (10), 3653–3668. https://doi.org/10.1111/1462-2920.14694.
Solomon, F., 2008. Impacts of metals on aquatic ecosystems and human health. Environment and Communities 14–19. http://hdl.handle.net/1773/16440.
Stauber, J., Davies, C., 2000. Use and limitations of microbial bioassays for assessing copper bioavailability in the aquatic environment. Environ. Rev. 8 (4), 255–301. https://doi.org/10.1139/er-8-4-255.
Taylor, M.J., Bentham, R.H., Ross, K.E., 2014. Limitations of using propidium monoazide with qPCR to discriminate between live and dead Legionella in biofilm samples. Microbiology Insights. https://doi.org/10.4137/mbi.s17723, 7, MBI. S17723.
Thomas, K.V., Brooks, S., 2010. The environmental fate and effects of antifouling paint biocides. Biofouling 26 (1), 73–88. https://doi.org/10.1080/08927010903216564.
Thorley, J., Schwarz, C., 2018. ssdtools: an R package to fit species sensitivity distributions. Journal of Open Source Software 3 (31), 1082. https://doi.org/10.21105/joss.01082.
Turner, S., Pryer, K.M., Miao, V.P., Palmer, J.D., 1999. Investigating deep phylogenetic relationships among cyanobacteria and plastids by small subunit rRNA sequence analysis. J. Eukaryot. Microbiol. 46 (4), 327–338. https://doi.org/10.1111/j.1550-7408.1999.tb04612.x.
USEPA. (2019). ECOTOX User Guide: ECOTOXicology Database System. Version 5.0. United States Environmental Protection Agency. http://cfpub.epa.gov/ecotox/ (accessed 27 March 2023).
Vaishampayan, P., Probst, A.J., La Duc, M.T., Bargoma, E., Benardini, J.N., Andersen, G. L., Venkateswaran, K., 2013. New perspectives on viable microbial communities in low-biomass cleanroom environments. The ISME Journal 7 (2), 312–324. https://doi.org/10.1038/ismej.2012.114.
Vandeputte, D., Kathagen, G., D'hoe, K., Vieira-Silva, S., Valles-Colomer, M., Sabino, J., Wang, J., Tito, R.Y., De Commer, L., Darzi, Y., 2017. Quantitative microbiome profiling links gut community variation to microbial load. Nature 551 (7681), 507–511. https://doi.org/10.1038/nature24460.
Vanwonterghem, I., Webster, N.S., 2020. Coral reef microorganisms in a changing climate. Iscience 23 (4), 100972. https://doi.org/10.1016/j.isci.2020.100972.
Vehtari, A., Gelman, A., Gabry, J., 2017. Practical Bayesian model evaluation using leave-one-out cross-validation and WAIC. Stat. Comput. 27 (5), 1413–1432. https://doi.org/10.1007/s11222-016-9696-4.
Vehtari, A., Gabry, J., Magnusson, M., Yao, Y., Bürkner, P. C., Paananen, T., & Gelman, A. (2023). loo: efficient leave-one-out cross-validation and WAIC for Bayesian models. R package version 2.6.*0* In https://mc-stan.org/loo/.
Wang, Y., Yan, Y., Thompson, K.N., Bae, S., Accorsi, E.K., Zhang, Y., Shen, J., Vlamakis, H., Hartmann, E.M., Huttenhower, C., 2021. Whole microbial community viability is not quantitatively reflected by propidium monoazide sequencing approach. Microbiome 9 (1), 1–13. https://doi.org/10.1186/s40168-020-00961-3.
Warne, M.St.J., Reichelt-Brushett, A., 2023. Pesticides and Biocides. In: Reichelt-Brushett, A. (Ed.), Marine Pollution–Monitoring, Management and Mitigation, 1 ed. Springer, pp. 155–184. https://doi.org/10.1007/978-3-031-10127-4.
Warne, M.St.J., Batley, G., van Dam, R., Chapman, J.R., Fox, D., Hickey, C., Stauber, J., 2018. Revised Method for Deriving Australian and New Zealand Water Quality Guideline Values for Toxicants – Update of 2015 Version. Prepared for the revision of the Australian and New Zealand Guidelines for Fresh and Marine Water Quality.
Webster, N.S., Webb, R.I., Ridd, M.J., Hill, R.T., Negri, A.P., 2001. The effects of copper on the microbial community of a coral reef sponge. Environ. Microbiol. 3 (1), 19–31. https://doi.org/10.1046/j.1462-2920.2001.00155.x.
Webster, N.S., Wagner, M., Negri, A.P., 2018. Microbial conservation in the Anthropocene. Environ. Microbiol. 20 (6), 1925–1928. https://doi.org/10.1111/1462-2920.14124.
Wickham, H., 2016. ggplot2: Elegant Graphics for Data Analysis. In (Version R package 3.4.0). Springer-Verlag, New York. https://ggplot2.tidyverse.org.
Yang, J., Xie, Y., Jeppe, K., Long, S., Pettigrove, V., Zhang, X., 2018. Sensitive community responses of microbiota to copper in sediment toxicity test. Environ. Toxicol. Chem. 37 (2), 599–608. https://doi.org/10.1002/etc.3980.
Yin, B., Crowley, D., Sparovek, G., De Melo, W.J., Borneman, J., 2000. Bacterial functional redundancy along a soil reclamation gradient. Appl. Environ. Microbiol. 66 (10), 4361–4365. https://doi.org/10.1128/AEM.66.10.4361-4365.2000.
Zhang, X., 2019. Environmental DNA shaping a new era of ecotoxicological research. Environ. Sci. Technol. 53 (10), 5605–5612. https://doi.org/10.1021/acs.est.8b06631.
Zhu, X.-W., Liu, S.-S., Qin, L.-T., Chen, F., Liu, H.-L., 2013. Modeling non-monotonic dose–response relationships: model evaluation and hormetic quantities exploration. Ecotoxicol. Environ. Saf. 89, 130–136. https://doi.org/10.1016/j.ecoenv.2012.11.022.